Received: 1 May 2019 | Revised: 27 November 2019 | Accepted: 4 February 2020

DOI: 10.1002/2050-7038.12359

RESEARCH ARTICLE

WILEY

Effects of harmonic pollution on salient pole synchronous generators and on induction generators operating in parallel in isolated systems

Wagner E. Vanço[1] | **Fernando B. Silva**[2] | **José M. M. de Oliveira**[3] | **José R. B. Almeida Monteiro**[1]

[1]Escola de Engenharia de São Carlos, Universidade de São Paulo, São Carlos, São Paulo, Brazil

[2]Departamento de Engenharia Elétrica, Universidade Federal de Ouro Preto, Instituto de Ciências Exatas e Aplicadas, João Monlevade, Minas Gerais, Brazil

[3]Faculdade de Engenharia Elétrica, Universidade Federal de Uberlândia, Campus Santa Mônica, Uberlândia, Minas Gerais, Brazil

Correspondence
Wagner E. Vanço, Escola de Engenharia de São Carlos, Universidade de São Paulo, São Carlos, São Paulo, Brazil.
Email: vanco@usp.br

Peer Review
The peer review history for this article is available at https://publons.com/publon/10.1002/2050-7038.12359.

Summary

This work presents a study of the disturbances caused by harmonic pollution in salient pole synchronous generators (SPSG) and induction generators, when operating in parallel in isolated systems. SPSG are known to operate with induction generators, since the excitation system of the synchronous generator is responsible for the voltage control on the island system. Due to the increase in the employment of power electronics, the loads take on a nonlinear behavior, where these become responsible for the generation of harmonics, due to the switching of electrical devices. Therefore, the analysis of the disturbances that these loads cause in generators, in this proposed and studied architecture, becomes essential. For the synchronous generator, there is also presented the analyses of the oscillations for voltages and currents on the *dq0* model, the currents induced on the damper winding, the disturbances on the load angle and on the field current. In terms of the induction generator, the voltage and current oscillations are also analyzed from the *dq0* model on the slip frequency. All the identified and quantified disturbances are oscillations on the electric variables, which possess a pulsating nature of frequencies 6ω, 12ω, and 18ω for the synchronous and induction generators, the oscillations of the sixth order

List of Symbols and Abbreviations: A, design constant of the induction machine winding; *abc*, a-b-c domain; AVR, automatic voltage regulator; DC, electrical energy of direct type; DFIG, doubly fed induction generators; *dq0*, direct-quadrature-zero transformation; DSTATCOM, distribution static synchronous compensator; EMF, electromotive force; *fmm*, magnetomotive force; fmm_h, magnetomotive force of harmonic order h; h, harmonic component; h_{max}, maximum harmonic order present in the waveform; i'_d, current in direct damping coil; i'_{dr}, direct axis rotor current; i'_{fd}, field winding current; i'_{q1}, current in quadrature damping coil; i'_{qr}, quadrature axis rotor current; I_1, maximum value of the fundamental component of the stator current; I_a, phase A current; i_{ds}, direct-axis stator current; IG, induction generator; I_h, maximum value of the harmonic component of the stator current; i_{qs}, quadrature axis stator current; K, machine winding design constant; RMS, root-mean-square; R_r, rotor resistance; R_s, stator resistance; s_1, slippage for the fundamental frequency; S1, switch 1; S2, switch 2; s_5, slippage for the fifth frequency; s_7, slippage for the seventh frequency; s_h, slippage for the harmonic order h; SPSG, salient pole synchronous generator; T''_d, direct axis short circuit subtransient time constant; T''_q, quadrature axis short circuit subtransient time constant; T'_d, direct axis short circuit transient time constant; T_1, electromagnetic torque due to the fundamental component; T_5, electromagnetic torque due to the fifth order harmonic component; $T_{6\omega}$, resulting oscillating portion of the electromagnetic torque; T_7, electromagnetic torque due to the seventh order harmonic component; T_{cc}, resulting portion of the continuous level of electromagnetic torque; T_e, resulting electromagnetic torque; THD, total harmonic distortion; THD_i, total harmonic distortion (current); THD_v, total harmonic distortion (voltage); TIG, three-phase induction generator; V_a, phase A voltage; v_{ds}, direct-axis stator voltage; v_{qs}, quadrature axis stator voltage; X''_d, direct axis subtransient reactance; X''_q, quadrature axis subtransient reactance; X'_d, direct axis transient reactance; X_d, direct axis reactance; X_l, leakage reactance; X_{lr}, rotor dispersion reactance; X_{ls}, stator dispersion reactance; X_m, magnetizing reactance; X_q, quadrature axis reactance; δ, load angle; Δ_ω, generated speed error; θ, spatial angle with origin in one of the stator phases; ω, synchronous speed; ω_m, mechanical speed of the rotor; ω_{ref}, synchronous reference speed; ω_{ref1}, asynchronous reference speed.

and its multiples, will be given in the harmonic slip frequency of their respective harmonic orders in positive and negative sequence. In this way, verification is made as to the appearance of high slippage on the rotor of the induction generator.

KEYWORDS

disturbances, harmonic effects, harmonic load, induction generator, nonlinear load, oscillations, power quality, salient poles, synchronous generator

1 | INTRODUCTION

Throughout the 20th century until the present moment, synchronous generators have remained the principal devices for electromechanical conversion used in large electric power systems around the world. In this case, large machines with a power of hundreds of Mega Volt-Ampère (MVA) constitute the generation base of hydroelectric, nuclear, or thermal power plants. Noteworthy is that the use of synchronous generators is not restricted only to the large electric power systems, its use in diesel generator groups is also widely used in applications in isolated systems. These generator groups are able to supply loads to isolated areas, where high cost places insurmountable difficulties upon the implementation of electric power transmission lines, as well as acting as an emergency unit for industries, hospitals, among others.[1,2]

However, the cost of synchronous generation is high, due to the constructive and preventive maintenance characteristics of the generator. On the other hand, the induction motor with squirrel cage rotor is widely applied in industry, where it is also used as a generator. Due to its robustness, simplicity, and relatively low cost, the induction motor with squirrel cage rotor has seen a wide-ranging use.[2]

Besides operating as a motor, the operation of the induction machine as a generator is currently gaining ground in the power scenario. In highlighting the operation of the squirrel cage induction generator, this needs to consume reactive power to function, which is derived from the electric network or capacitor bank when connected to the electric system or supplied exclusively by the capacitor bank when operating in isolation.

With the emphasis placed upon the operation of isolated electric systems, one notes that the synchronous generation used in diesel generator groups can be complemented with asynchronous generation by means of squirrel cage induction generators. Due to advantages highlighted and brought by this type of generation, especially in terms of the question of maintenance and robustness found in asynchronous generation.

In addition, emphasis is given to poor voltage regulation, which is a principal disadvantage when using induction generators; however, this is compensated by the operation in parallel with synchronous generators. These possess the capacity to maintain the terminal voltage of the set constant, controlled by its excitation system. Therefore, one notes that the characteristics of these two types of generators are complementary, thus bringing significant advantages to a generation system constituted of these two machines.

It is noted that currently diesel generator groups are subject to supplying all kinds of loads. Among such emphasis is given to nonlinear loads, mainly present in residential, industrial, and commercial users, in the form of air conditioning, compact lamps, and computers, among others. The growth of these loads in consumer demand has intensified due to the numerous applications that power electronics provides. The switching of these electronic devices is responsible for the generation of harmonics, thus causing distortions to the current and consequently to the voltage on a specific electric system.

2 | BIBLIOGRAPHIC REVISION, SCIENTIFIC RELEVANCE AND SIGNIFICANCE

2.1 | Bibliographic revision

Presented in this section are studies that refer to synchronous generators and nonlinear loads, of which the following are highlighted:

With the aim of discussing the impacts of spatial harmonics in rotating machines, a study is presented in Reference 3 concerning the calculation of the induced EMF, step factor, and distribution factor taking into account the effect of harmonics in the calculation of the total harmonic distortion of the voltage generated. In Reference 4, the study of the distortion on the waveform for voltage and current is analyzed in an isolated synchronous generator, which supplies a nonlinear load, where the synchronous generator uses an exciter supplied by a bridge rectifier connected to the machine terminal.

In Reference 5, a description is given for a synchronous generator model that includes harmonic impedances on the impedance array of the equivalent circuit of the machine. In Reference 6, a synchronous generator model is highlighted on the *abc* domain, which considers spatial harmonics. In this case, a *park* transformation is applied to the fundamental flow of the stator with the aim of calculating the fundamental voltage generated, as well as the load angle.

In Reference 7, an investigation is made into harmonics caused by an internal fault in the synchronous generator, the model also considers the spatial harmonics caused by the distribution of the machine windings. Another relevant aspect is addressed in Reference 8, which presents the harmonic effect over the voltage regulation on synchronous generators in a nonsinusoidal regime, through an analysis of different levels of harmonic distortion produced by the nonlinear load.

A study of mechanical resonance with the sixth harmonic and its multiples is presented in Reference 9, in which consideration is given to a distortion of relatively low current, with a comparison made to the actual situation of the harmonic distortion encountered in isolated synchronous generators.

In dealing with induction generators that operate under the influence of harmonic distortions, with nonlinear loads and control techniques used to mitigate these distortions, one finds various studies on the subject of the operation of doubly fed induction generators (DFIG), which operate on windfarms connected to or isolated from the network. Additionally, in less number, some studies are presented for three-phase induction generators (TIG) of the squirrel cage type under nonlinear loads. Following this line, the following studies can be highlighted:

In Reference 10, an analysis technique that covers harmonic resonance problems on windfarms connected to a power electric system is shown, where DFIG are used. In Reference 11, a study is presented for current and voltage harmonic flows, which are generated by inter-harmonics and the effect caused by the level of harmonic emissions from a windfarm.

In Reference 12, a study aimed at harmonic emission measurements vs active power is presented for a set of three wind turbines composed of two DFIG and a synchronous generator.

In Reference 13, a new method is proposed for the detection of the islanding of wind generators that are connected to the network, based on the calculation of the value of the total current distortion of the generator units composed of DFIG. In Reference 14, the authors investigate the harmonic frequency values generated in a system composed of DFIG and its converter.

In Reference 15, a new control technique is presented for a distribution static synchronous compensator (DSTATCOM) In this case, this equipment is connected to an isolated distribution system supplied by a windfarm with DFIG. The application of this new control technique called optimized $Icos\varphi$ allows the DSTATCOM to mitigate the current THD level present in this system.

Also, aiming at the compensation of current harmonic distortions, in this particular case those arising from nonlinear loads, the proposal is put forward in Reference 16 for a method using the multiple axis reference frame theory, utilizing DFIG. The most significant low order harmonics to be compensated are calculated using a harmonic observer of multiple axis reference frame.

Through the consideration that voltage harmonic pollution present in an electric power system can introduce current harmonics onto the stator of DFIG, which are potentially capable of affecting the quality of the energy generated, one finds in Reference 17 a current controller specific to DFIG generators for eliminating the impacts of harmonics of low voltage order.

In Reference 18, emphasis is given to the analysis of harmonic distortions in current waveforms arising from electronic loads connected to a self-excited induction generator.

In Reference 19, an experimental analysis is presented for the harmonic distortions in self-excited induction generators, the analysis is performed for nonconventional energy systems, onto which a self-excited induction generator is connected to a frequency inverter, in order to supply a particular load.

2.2 | Scientific importance

Highlighted here is that different to studies presented in the literature, the theme covered herein investigates the various effects that the harmonic voltage and current distortions cause in both machines, when these are operating in parallel in an isolated system, which supplies a nonlinear load.

In this way, there arises the importance behind performing an operational study in isolated form of a synchronous generator in parallel with an induction generator, supplying nonlinear loads, which aims at studying the impacts and disturbances that harmonic pollution causes in generators.

Emphasized here is that the operation in parallel of these two types of generators, besides the application in diesel generator groups, can also be employed in a number of endeavors such as small hydroelectric plants, in biomass with greater focus on cogeneration of electric energy using biogas produced from organic residues.

In addition, consideration should be given, in isolated operation, to the level of short-circuit on the terminals of these machines (synchronous and induction generators) which is many times lower than on a bus of an electric power system. Thus, emphasis is placed on the susceptibility of generators faced with harmonic distortions imposed by these loads. Therefore, the effects of the current harmonic distortions imposed by the nature of the nonlinear loads manage to distort the generated voltage waveform, besides the appearance of undesired effects, which contribute to decreasing the yield and working life of the generators.

An important contribution of this article is based on the identification of the high slippage on the rotor of the induction generator. In the literature studies are presented for a similar effect that occurs in induction motors when fed with distorted voltages, where emphasis is placed upon the decrease in torque in the machine. In the study of induction motors, this effect is classified as the crawling effect. However, the present literature lacks investigations on these high slippage occurrences in induction generators, with there still no description of the effect or classification being given in the literature. As such, this article presents this contribution, which is to identify and classify the harmonic orders responsible for creating these high slippage occurrences on the rotor of the induction generator.

3 | MATHEMATICAL MODELLING, HARMONICS IN SYNCHRONOUS, AND INDUCTION MACHINES

The equations for the synchronous machine with salient poles and for the squirrel cage rotor induction machine are presented in Reference 20.

3.1 | Harmonic distortions in synchronous machines

The nonlinear loads are responsible for the generation of harmonics, due to the switching of the devices that employ power electronics. The operation of the machine in nonsinusoidal steady state has a direct influence on yield, power factor, heating, and instabilities. Such abnormalities reflect upon the increase in electric losses (thermal and dielectric stress), as well as mechanical damage, factors which are disadvantageous when analyzed from the electric and economical point of view.

Harmonics cause losses on the stator winding, these losses on the stator copper can be estimated by the increase in ohmic loss in relation to the sinusoidal scheme, in the squared order of the THD for the (THD_i^2) current.[3] Such a fact contributes to the increase in temperature on the machine windings, besides increasing dielectric stress on the insulating materials, due to the increase in the effective voltage values.[21] Emphasis is also given to the core losses, being that the harmonic components lead to an increase in losses caused by hysteresis and in the losses caused by parasitic currents, where the losses caused by parasitic currents are greater than those caused by hysteresis.[3]

The supportability values adopted for the synchronous machines, the THD_i value, which calculates the value of the total current harmonic distortion, should be at maximum 5%, and is given by[22]:

$$THD_i(\%) = \frac{\sqrt{\sum_{h=2}^{h_{max}} {I_h}^2}}{I_1} \times 100 \leq 5\% \quad (1)$$

The harmonic components which cause oscillations to the torque on the axis of synchronous generators were investigated, these are represented in the form of oscillating electromagnetic torque, besides the harmonic order voltage induction on the rotor of the generator (on the field and damping windings)

Such phenomena are generated by the interactions between the magnetic field in the fundamental frequency and the harmonic orders present on the stator, being that the current circulation of the fifth and seventh harmonics result

in a continuous torque of sixth order harmonic on the rotor of the synchronous machine. As these values can coincide with the natural frequency of the coupling (turbine + rotor), such a situation can cause mechanical fatigue of the material constituting the axis, and as such lead to severe damage to the generator.[9,23]

Thus, for a synchronous generator that supplies a nonlinear load, the combined sum of the temporal harmonic orders due to the nonsinusoidal currents that circulate in the stator of the machine result in a spatial distribution of magnetomotive force between the stator and the rotor of the synchronous generator, as shown by:

$$fmm = \sum fmm_h \tag{2}$$

$$fmm_h = \sum KI_h \begin{bmatrix} \cos(\theta)\cos(h\omega t) + \cos\left(\theta - \frac{2\pi}{3}\right)\cos\left[h\left(\omega t - \frac{2\pi}{3}\right)\right] + \\ \cos\left(\theta + \frac{2\pi}{3}\right)\cos\left[h\left(\omega t + \frac{2\pi}{3}\right)\right] \end{bmatrix} \tag{3}$$

By substituting h in Equation (3) for the values of odd numbered orders, one has:

$$h = 1 \rightarrow mmf_1 = \frac{3}{2}KI_1\cos(\theta - \omega t), \text{ sequence } (+) \tag{4}$$

$$h = 3 \rightarrow mmf_3 = 0, \text{ sequence } (0) \tag{5}$$

$$h = 5 \rightarrow mmf_5 = \frac{3}{2}KI_5\cos(\theta + 5\omega t), \text{ sequence } (-) \tag{6}$$

$$h = 7 \rightarrow mmf_7 = \frac{3}{2}KI_7\cos(\theta - 7\omega t), \text{ sequence } (+) \tag{7}$$

where, fmm, magnetomotive force (A.e); fmm_h, magnetomotive force of harmonic order h (A.e); h, harmonic component; K, machine winding design constant; I_h, maximum value of the harmonic component of the stator current (A); θ, spatial angle with origin in one of the stator phases (degrees); ω, Synchronous speed (rad/s).For the remaining harmonic orders, by changing the value of the h index, one has: $h = 9$, which possesses the same phase sequence of $h = 3$; $h = 11$, which possesses the same phase sequence as $h = 5$; $h = 13$, which possesses the same phase sequence of $h = 1$, and so on. However, these will successively produce multiple sixth order components (12ω, 18ω, ...).

The equations described in (2) to (7) provide a physical representation of thefmm (magnetomotive force) rotating at a constant angular speed with a positive and negative sequence in relation to the stator of the machine as presented in Figure 1, together with the fmm_h components, arising from other harmonic orders starting out with the fifth.

The seventh order harmonic currents, when circulating through the stator windings generate a rotating magnetic field, for which the speed is seven times the value of the synchronous speed. These seventh order harmonic currents are of positive sequence, being these that will produce a magnetic field, which spins in the same direction as the rotor. This results in a magnetic field that cuts through the rotor windings with a speed of ($7\omega - \omega = 6\omega$), that is, six times the synchronous speed, which will lead to the induction of currents of the seventh harmonic on the rotor windings.

Similarly, the currents of the fifth harmonic order, when circulating on the stator windings generate a rotating magnetic field five times the value of the synchronous speed. These harmonic currents are of negative sequence, and will produce a magnet field that spins in the opposite direction to the rotor, thus resulting in a magnetic field that cuts the rotor windings with a speed of ($\omega - [-5\omega] = 6\omega$), resulting in an induced current of the sixth harmonic order.[24]

3.2 | Harmonic distortions in induction machines

In similar fashion to Equation (3), the equation for the total magnetomotive force is described in Reference 25, for evaluating the effect of the temporal harmonics in induction machines, which is given by:

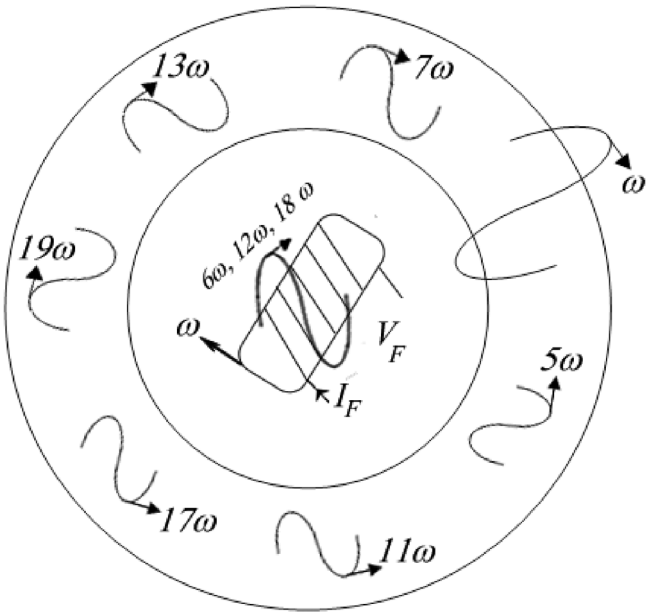

FIGURE 1 Magnetomotive force components. Source: Extracted from Reference 24

$$fmm = \sum \frac{3}{2} A I_h \cos(\theta \pm h\omega t) \tag{8}$$

where, *fmm*, magnetomotive force (A.e); *h*, harmonic component; A, design constant of the machine winding; I_h, maximum value for the harmonic component stator current (A); θ, spatial angle originating in one of the stator phases (degrees); ω, synchronous speed (rad/s).

By considering (8) as the positive value for harmonic components of negative sequence, and the negative value for harmonic components of positive sequence. As found in the synchronous machine, the harmonic currents of the fifth and seventh orders will produce torque on the frequency of 5ω and 7ω, as illustrated in Figure 2. The phasorial sum produces a continuous electromagnetic torque, developed by the fundamental component and added to a pulsating torque of 6ω, which results in a difference of the magnetic field speeds produced by these components ($\omega - [-5\omega] = 6\omega$) and ($7\omega - \omega = 6\omega$)

Equation (9) provides a better explanation to this electric phenomenon, taking into consideration the analysis for the operation of the induction generator.

$$T_e = T_1 + T_5 + T_7 = T_{cc} + T_{6\omega} \tag{9}$$

where, T_e, resulting electromagnetic torque (N.m); T_1, electromagnetic torque due to the fundamental component (N.m); T_5, electromagnetic torque due to the fifth order harmonic component (N.m); T_7, electromagnetic torque due to the seventh order harmonic component (N.m); T_{cc}, resulting portion of the continuous level of electromagnetic torque (N.m); $T_{6\omega}$, resulting oscillating portion of the electromagnetic torque (N.m).

By including the harmonic components *h*, of odd numbered pairs, the equation for electromagnetic torque, can be represented mathematically by (10)

$$T_e = T_{cc} + \sum \frac{T_{(h\pm1)}}{2} \tag{10}$$

Once again, the positive value is for the harmonic components of negative sequence, and the negative value for the harmonic components of positive sequence. Therefore, the resulting electromagnetic torque will be the sum of the continuous electromagnetic torque, plus the sum of the multiple pulsating electromagnetic torque for the frequency of 6ω, similarly to that previously analyzed.

The currents on the rotor, as well as the squared and right axis voltages and currents are in the sliding frequency, when in sinusoidal mode. Through an analysis of the operation in nonsinusoidal mode, there will exist slippage in each

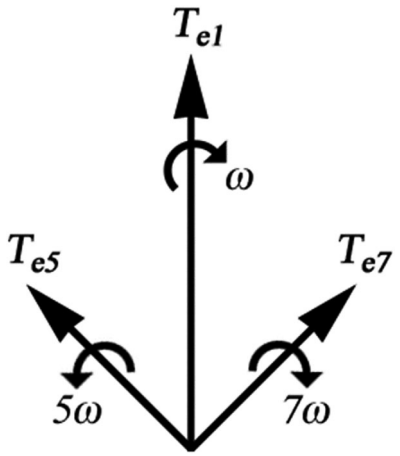

FIGURE 2 Graph representation of the phasor for the torque superposition due to the harmonic components. Source: Adapted from Reference 25

harmonic order. Thus, the slippage for the fundamental frequency, as well as for the fifth and seventh portions, can be given respectively by (11) to (13).[25]

$$s_1 = \frac{\omega - \omega_m}{\omega} \tag{11}$$

$$s_5 = \frac{5\omega + \omega_m}{\omega} \tag{12}$$

$$s_7 = \frac{7\omega - \omega_m}{\omega} \tag{13}$$

where, ω_m, mechanical speed of the rotor (rad/s).

For the odd numbered components of order$h$, one has the following equation:

$$s_h = \frac{h\omega \pm \omega_m}{\omega} \tag{14}$$

with this being the positive value for harmonic components of negative sequence, and the negative value for harmonic components of positive sequence.

The relationship between the slippage due to the harmonic orders (s_h) regarding the fundamental slippage (s_1) is given by:

$$s_h = \frac{h\omega - \omega_m}{\omega} = \frac{\omega - \omega_m}{\omega} + \frac{(h-1)\omega}{\omega} \tag{15}$$

with,

$$s_1 = 1 - \frac{\omega_m}{\omega} \tag{16}$$

thus,

$$s_h = 1 - \frac{\omega_m}{\omega} + h - 1 = h - (1 - s_1) \tag{17}$$

$$s_h = s_1 + (h-1) \tag{18}$$

For those harmonic orders of positive sequence, one uses Equation (18), while Equation (19) is used for harmonic orders of negative sequence.

$$s_h = -s_1 + (h+1) \tag{19}$$

4 | METHODOLOGY FOR THE EXPERIMENTAL PROCEDURE

The experimental tests were performed on a laboratory test bench, which was composed of a salient pole synchronous generator (SPSG), and by a TIG, both operated by two DC motors. The representative diagram for the experimental procedure performed with the two generators is shown in Figure 3.

The first step is to start up the DC motor, in order that these remain at the synchronous speed, in no-load and shortly thereafter close switch S1, in a way that the asynchronous machine performs the start up as a motor. One starts up the DC motor coupled to the induction generator (the DC motor should spin in the same direction as the induction machine) The speed of the induction generator is adjusted in order that it is at a faster speed than that of the rotating field of its stator, and shortly after, close switch S2, placing the load on the generators. If the induction machine is powered, it is necessary to increase slippage without the load, that is, turn off the load (opening switch S2), thus increasing the mechanical speed of the induction generator to a speed value slightly higher than that of the synchronous generator in no-load.

If the induction machine behaves as a generator when the closing of S2 occurs, one adjusts the frequency of the system to 60 Hz, through use of the speed control of the DC machines. The controlling of the terminal voltage is performed by means of the excited control circuit of the synchronous generator, absorbing or supplying reactive power depending on load variation, thus guaranteeing values that are always close to the nominal voltage. The three-phase bench is designed as in Reference 26.

Figure 4 shows the experimental bench mounted for performing the experiment. As noted in the following images, the induction generator is on the left, while the synchronous generator is to the right, both moved by a DC motor. The excitation control for the synchronous generator is found to the right.

4.1 | Results of the experimental procedure

In the architecture of the joint operation of the synchronous generator with the induction generator, when a nonlinear load is in isolated operation, one obtains oscillographic readings at the indicated points (meter-phase readings) as in Figure 3. This test is necessary in order to demonstrate posteriorly, in the computer simulation, that the oscillations present in the electric variables of the generators, when supplying nonlinear loads, are significant.

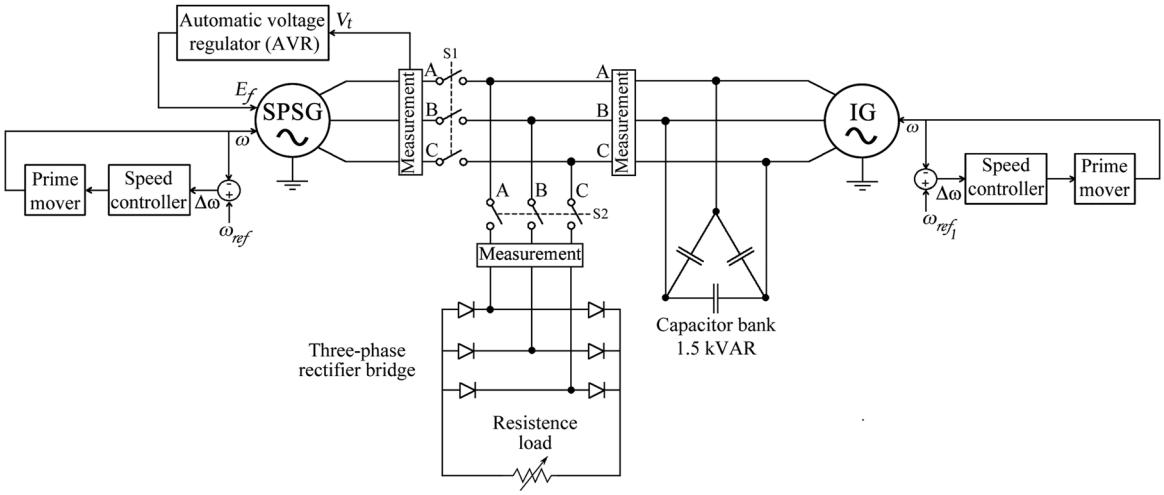

FIGURE 3 A representative diagram of the experimental work bench for the synchronous and induction generators, supplying a three-phase nonlinear load

The phase voltage waveform of the isolated system or on the coupling point (between the generators and the load) is illustrated in Figure 5. Table 1 shows the decomposition of the phase voltage (peak values) waveform of the isolated system.

The phase current waveform on the synchronous generator is illustrated in Figure 6. Table 2 shows the decomposition of the current (peak values) waveform from the synchronous generator.

The phase current waveform generated by the induction generator obtained from the capacitor bank terminals is shown in Figure 7. Table 3 shows the decomposition of the current (peak values) waveform from the induction generator.

The current waveform on the nonlinear load is illustrated in Figure 8. Table 4 shows the decomposition (peak values) of the waveform on the nonlinear load.

The RMS voltage values for the isolated system and current on the synchronous generator are obtained in accordance with Reference 21. Through the data presented on Tables 1 and 2, one obtains:

The RMS voltage for the isolated system: 230.2424 (V).

The RMS current for the synchronous generator: 1.7084 (A).

One obtains the RMS current values on the induction generator and the nonlinear load with the data present on Tables 3 and 4, respectively.

The rms current on the induction generator: 1.5264 (A).

The rms current on the nonlinear load: 2.9308 (A).

5 | COMPUTER SIMULATION METHODOLOGY

The data and parameters of the SPSG are shown through Tables 5 and 6. For the squirrel cage induction generators, the data and parameters can be found on Table 7.

In the computational simulation of the generators, supplying a nonlinear load, the following procedures were defined on Table 8, according to the representative diagram of Figure 3.

The computer simulation used the data from the generators obtained by means of experimental tests, with the aim of representing, in the most natural way possible, the operation of these machines.

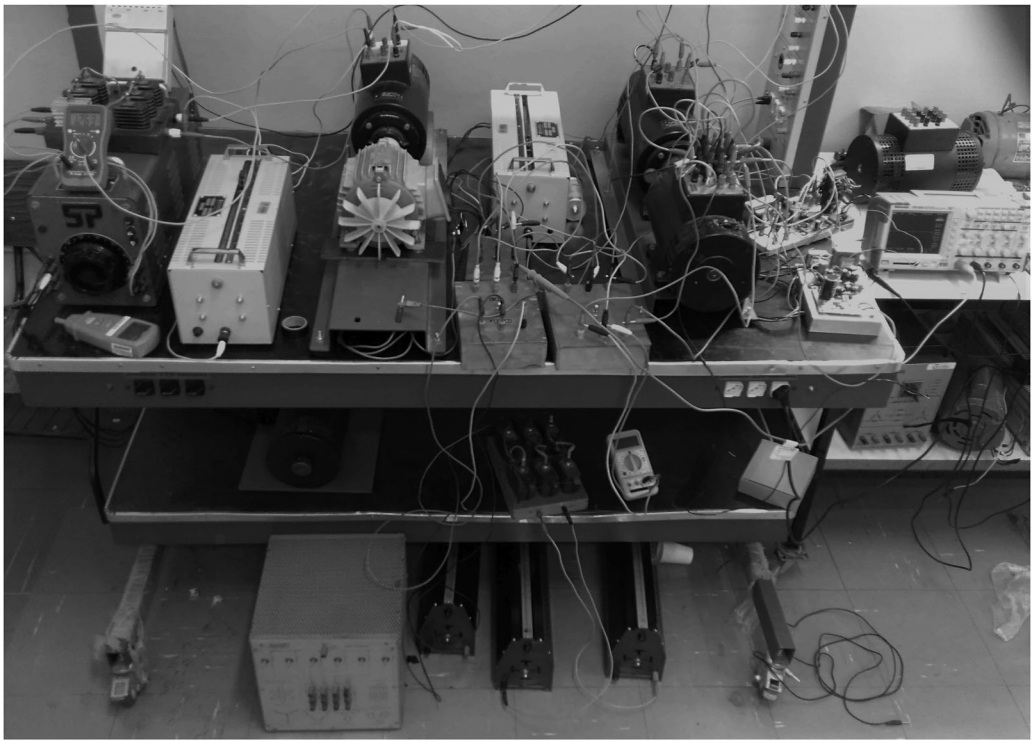

FIGURE 4 Experimental bench mounting

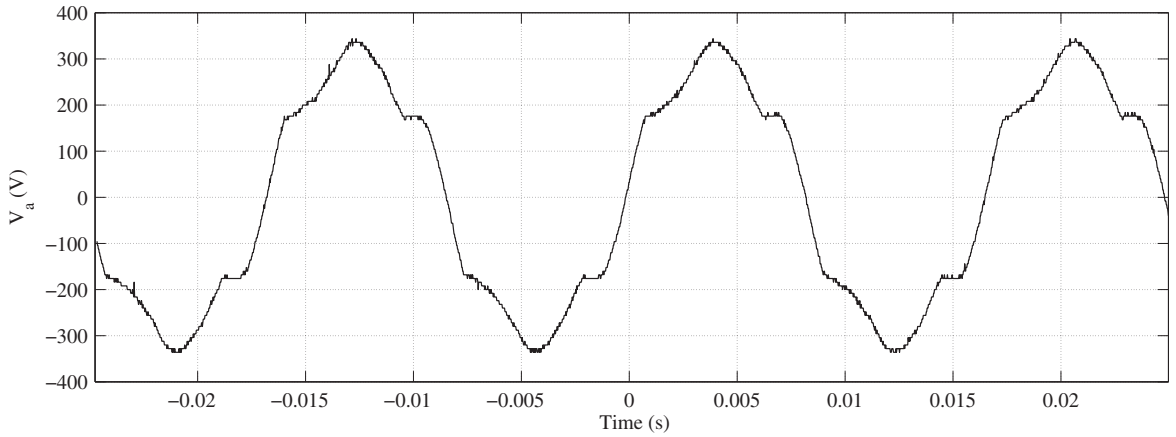

FIGURE 5 Phase voltage generated from the isolated system (at the coupling point)

TABLE 1 Decomposition of the phase voltage waveform from the isolated system

Approximated $THD_V = 12.764\%$							
DC	**1st**	**3rd**	**5th**	**7th**	**9th**	**11th**	**13th**
0.753	314.989	9.434	37.264	10.066	2.393	4.186	1.856
15th	**17th**	**19th**	**21st**	**23rd**	**25th**	**27th**	**29th**
0.855	1.672	1.125	0.422	0.749	0.578	0.170	0.383

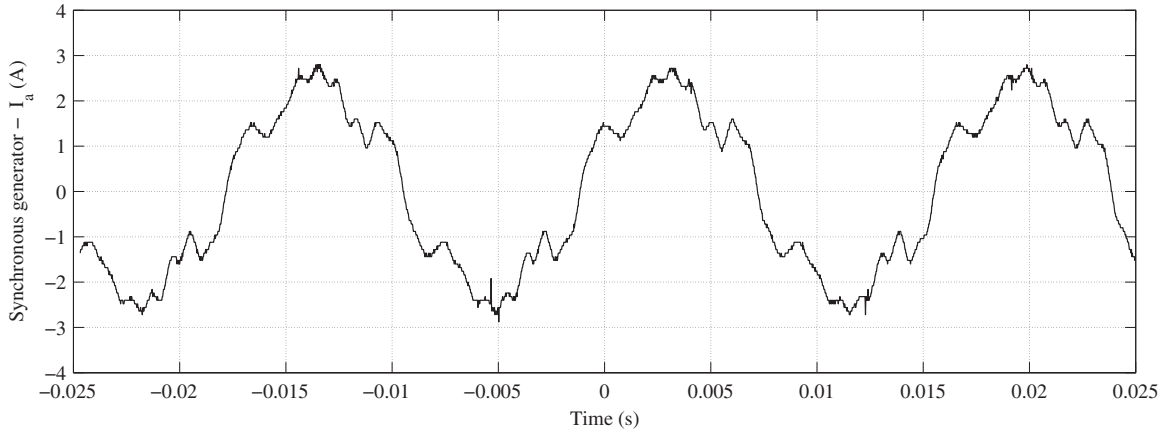

FIGURE 6 Phase current generated by the salient pole synchronous generator

TABLE 2 Decomposition of the phase current waveform from the synchronous generator

Approximated $THDi = 20.038\%$							
DC	**1st**	**3rd**	**5th**	**7th**	**9th**	**11th**	**13th**
0.036	2.369	0.015	0.403	0.201	0.008	0.021	0.021
15th	**17th**	**19th**	**21st**	**23rd**	**25th**	**27th**	**29th**
0.002	0.115	0.083	0.020	0.007	0.001	0.002	0.005

5.1 | Simulation results

The voltage waveforms from the isolated system and the phase current generated by the synchronous generator, when supplying a nonlinear load, are presented in Figure 9.

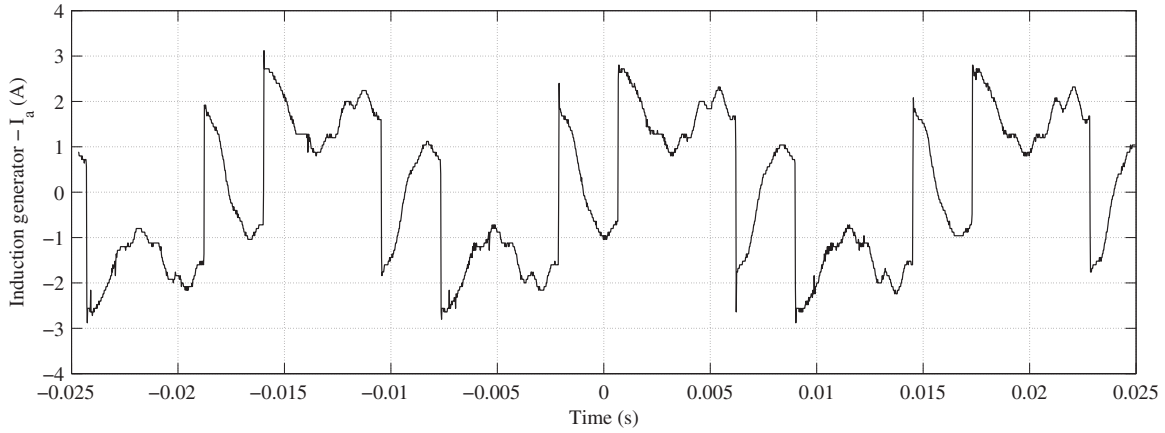

FIGURE 7 Phase current generated by the induction generator

TABLE 3 Decomposition of the phase current waveform of the induction generator

Approximated *THDi* = 92.785%							
DC	**1st**	**3rd**	**5th**	**7th**	**9th**	**11th**	**13th**
0.036	1.583	0.054	1.188	0.614	0.036	0.395	0.269
15th	**17th**	**19th**	**21st**	**23rd**	**25th**	**27th**	**29th**
0.027	0.168	0.170	0.049	0.185	0.127	0.030	0.145

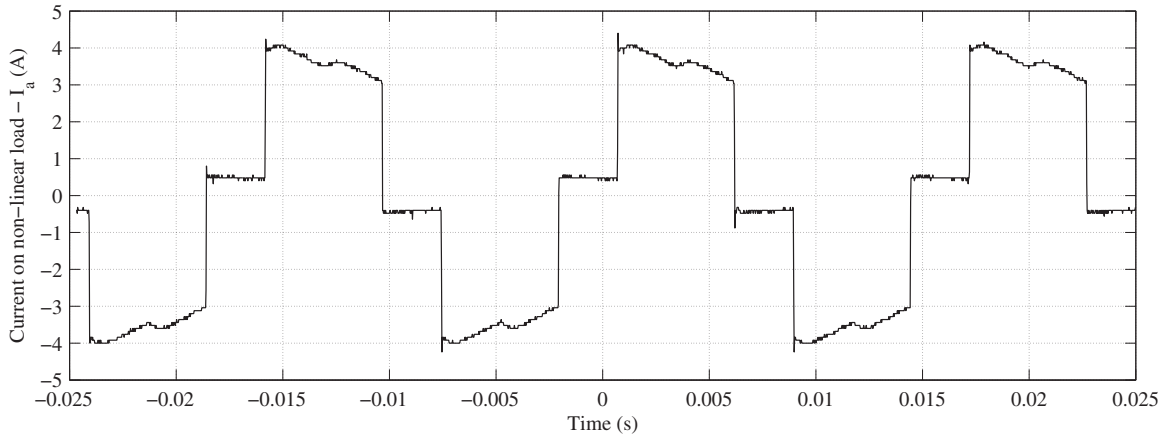

FIGURE 8 Current on the nonlinear load

TABLE 4 Decomposition of the phase current waveform on the nonlinear load

***Approximated THDi* = 29.951%**							
DC	**1st**	**3rd**	**5th**	**7th**	**9th**	**11th**	**13th**
0.025	3.975	0.075	0.872	0.492	0.065	0.391	0.239
15th	**17th**	**19th**	**21st**	**23rd**	**25th**	**27th**	**29th**
0.064	0.245	0.155	0.058	0.180	0.101	0.057	0.141

Tables 9 and 10 present the decomposition (in peak values) of the voltage waveforms for the isolated system (coupling point of the island system) and the current of the SPSG, respectively.

The RMS voltage values for the isolated system, the current on the synchronous generator, induction and for the nonlinear load are obtained through the data present on Tables 9–11, and 12, respectively.

TABLE 5 Data for the synchronous generator

Parameters	Values
Nominal voltage—YY	380 (V rms)
Nominal (full-load) current—YY	2.3 (A rms)
Nominal power	1.5 (kVA)
Nominal power factor	0.8
Nominal efficiency	0.85
Poles	4
Frequency	60 (Hz)
Moment of inertia	0.00928 [kg.m^2]
Constant of inertia	0.11 [s]
Isolation	A

TABLE 6 Parameters for the synchronous generator

Parameters	Values
Stator resistance	0.107 (pu)
Direct axis reactance, X_d	1.83 (pu)
Quadrature axis reactance, X_q	1.124 (pu)
Direct axis transient reactance, $X^{'}_{d}$	0.312 (pu)
Direct axis subtransient reactance, $X^{''}_{d}$	0.176 (pu)
Quadrature axis subtransient reactance, $X^{''}_{q}$	0.111 (pu)
Leakage reactance, X_l	0.263 (pu)
Direct axis short circuit transient time constant, $T^{'}_{d}$	17.60 (ms)
Direct axis short circuit subtransient time constant, $T^{''}_{d}$	5.30 (ms)
Quadrature axis short circuit subtransient time constant, $T^{''}_{q}$	5.25 (ms)

TABLE 7 Data and parameters for the induction generator

Parameters	Values
Nominal power	1 (cv)
Nominal voltage	380/220 (V)
Nominal (full-load) current	2.0/3.5 (A)
Connection	Y/Δ
Poles	4
Nominal power factor	0.7
Nominal efficiency	0.802
Frequency	60 (Hz)
Stator resistance, R_s	5.6 (Ω)
Rotor resistance, R_r	10.0 (Ω)
Magnetizing reactance, X_m	149.84 (Ω)
Stator dispersion reactance, X_{ls}	9.16 (Ω)
Rotor dispersion reactance, X_{lr}	13.47 (Ω)
Moment of inertia	0.0029 (kg.m^2)

RMS voltage for the isolated system: 224.31 (V).
RMS current for the synchronous generator: 2.00 (A).
RMS current for the induction generator: 1.6065 (A).
RMS current on the nonlinear load: 2.895 (A).

TABLE 8 The procedures performed in the simulation

Time (s)	Switching (procedures)
0	System start-up. Simulation initiation.
1	Turn on switch S1, synchronous generator performs motor start-up of no-load induction.
3	Increase the speed of the asynchronous machine above the synchronous speed, in order that it operates as a generator.
3.1	Trigger switch S2, the synchronous generator operates in parallel with the induction generator, supplying the nonlinear load.
10	Turn off the system. End of simulation.

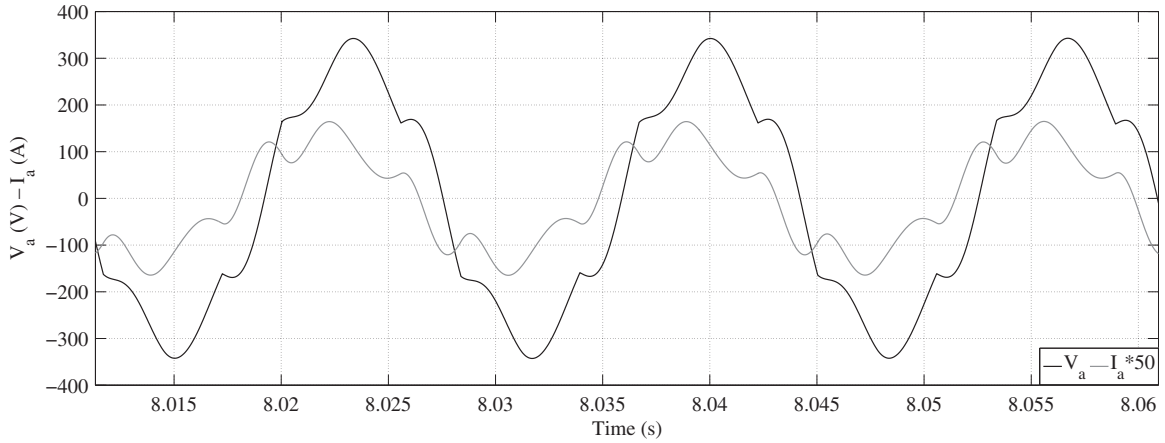

FIGURE 9 Voltage on the coupling point of the isolated system and the phase current generated by the synchronous generator

TABLE 9 Decomposition of the voltage waveform for the isolated system

Approximated $THD_V = 13.07\%$							
DC	**1st**	**3rd**	**5th**	**7th**	**9th**	**11th**	**13th**
0.08	314.55	0.11	38.93	12.2	0.04	3.87	2.38
15th	**17th**	**19th**	**21st**	**23rd**	**25th**	**27th**	**29th**
0.01	1.47	1.07	0.02	0.78	0.6	0.02	0.48

TABLE 10 Decomposition of the phase current waveform for the synchronous generator

Approximated $THDi = 27.21\%$							
DC	**1st**	**3rd**	**5th**	**7th**	**9th**	**11th**	**13th**
0	2.73	0	0.71	0.21	0	0.03	0.02
15th	**17th**	**19th**	**21st**	**23rd**	**25th**	**27th**	**29th**
0	0.01	0.01	0	0	0	0	0

The voltage waveforms for the isolated system and for the phase current generated by the induction generator, when supplying a nonlinear load are presented in Figure 10. Table 11 shows the decomposition (in peak values) of the current wave from the induction generator on the terminals of the three-phase capacitor bank.

The voltage waveforms for the isolated system and for the current on the nonlinear load are shown in Figure 11. Table 12 shows the decomposition (in peak values) of the current waveform for the nonlinear load.

TABLE 11 Decomposition of the phase current waveform for the induction generator

Approximated *THDi* = 105.21%							
DC	**1st**	**3rd**	**5th**	**7th**	**9th**	**11th**	**13th**
0	1.58	0	1.37	0.67	0.01	0.37	0.26
15th	**17th**	**19th**	**21st**	**23rd**	**25th**	**27th**	**29th**
0.01	0.22	0.17	0.01	0.16	0.13	0.01	0.12

TABLE 12 Decomposition of the phase current waveform on the nonlinear load

Approximated *THDi* = 26.47%							
DC	**1st**	**3rd**	**5th**	**7th**	**9th**	**11th**	**13th**
0	3.97	0.01	0.7	0.47	0.01	0.33	0.24
15th	**17th**	**19th**	**21st**	**23rd**	**25th**	**27th**	**29th**
0.01	0.21	0.17	0.01	0.15	0.13	0.01	0.12

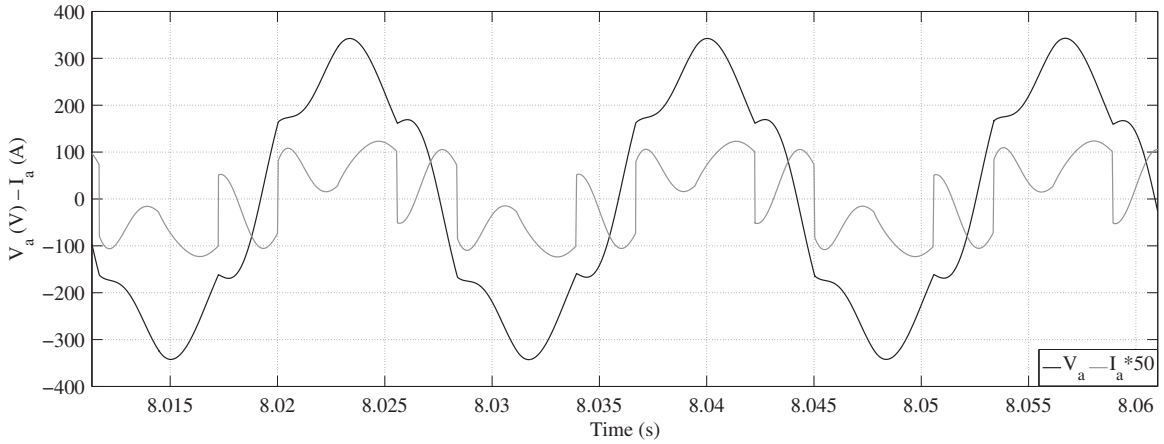

FIGURE 10 Voltage on the coupling point of the isolated system and phase current generated by the induction generator

6 | THEORETICAL–EXPERIMENTAL COMPARATIVE

By performing the comparison between the simulated data for the load with the reading obtained in the experimental trial, one notes proximity in the RMS value of the current for the nonlinear load used, besides the harmonic current distortions being of close approximation. The current distortion shows an acceptable error between the practical and simulation trials, among the harmonic components, for the load, synchronous and induction generator.

In the nonlinear load, the fact of the values for some simulated harmonic components possess a slight difference, in the aspects dealt with in the experiment for voltage and current, is due to difficulty in the precision to model or represent in the simulation the harmonic or nonlinear load. This occurs due to the internal induction and resistance values of the diodes, with values added from the resistance and capacitance snubber. These last two parameters are extremely sensitive to the nonsinusoidal characteristics imposed on the generators. The three-phase rectifier model is ideal and simplified, as such, small differences in the voltage harmonic components of the isolated system and in the currents generated by the generators are present in the theoretical-experimental comparison. This difference is acceptable between the obtained experimental and simulated decompositions (Tables 4 and 12)

In terms of the theoretical-experimental comparison for the current generated by the synchronous generator, this possesses a spatial distortion (spatial harmonics) due to being a synchronous generator from a simple didactic workbench. The phasorial sum of the temporal harmonics produced by the nonlinear load and by the spatial harmonics, generated by the constructive aspect of the machine, result in the difference of the harmonic components found on Tables 2 and 10.

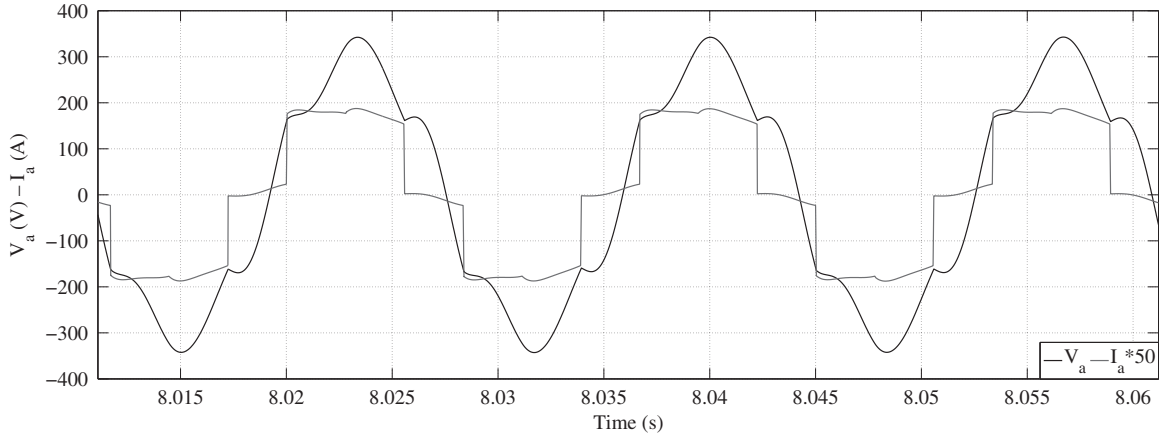

FIGURE 11 Voltage on the coupling point of the isolated system and current on the nonlinear load

In general, induction machines possess low distortions by spatial harmonics, due to the construction being optimized on the construction line, as the induction generator is nothing more than an induction motor with a squirrel cage rotor. It is for this reason that the values are closer than the synchronous generator, as seen through the values on Tables 3 and 11.

It should be borne in mind that the differences between the harmonic components in the isolated system are due to the fact that the simulations are based on ideal generator-load models, and more specific models would have to be used to reduce theoretical-experimental errors. Thus, one would need models envisaged on one that contemplates the harmonics produced by the constructive aspects of the generators (magnetic saturation and spatial harmonics), and also a model not ideal for nonlinear loading.

As previously explained, the values obtained between the practical and simulated trials are acceptable values, through this comparison, an analysis is made of the oscillations on the electrical variables on the SPSG and the induction generator with a squirrel cage rotor.

7 | EFFECTS FROM HARMONIC POLLUTION ON THE GENERATORS: ANALYSIS OF THE OSCILLATIONS

7.1 | SPSG

The developed electromagnetic torque and the harmonic spectrum of the electromagnetic torque from the synchronous generator are presented in Figure 12. As the system is nonsinusoidal, the electromagnetic torque has a pulsating nature.

Here DC means the continuous component, which is the value of the electric variable in its unit value, and the THD means the total harmonic pollution due to these cited oscillations. The values are plotted in percentages in relation to the continuous component.

The oscillation of the synchronous generator load angle and its respective harmonic spectrum are illustrated in Figure 13.

The quadrature and direct axis stator voltage and respective harmonic spectra are shown in Figures 14 and 15, respectively.

The quadrature and direct axis stator current and respective harmonic spectra are shown in Figures 16 and 17, respectively.

The field current or synchronous generator excitation of the synchronous generator for nonsinusoidal steady state and its respective spectrum illustrated through Figure 18.

The currents induced on the damping windings and their respective quadrature and direct harmonic axis spectra, due to harmonic pollution, are shown above in Figures 19 and 20, respectively.

Therefore, through an analysis of Figures 12 to 20, one notes the presence of oscillations in the electric variables of the synchronous generator, when this supplies a nonlinear load. The sixth harmonic component is predominant due to the fifth and seventh harmonic components being greater than the components that generate the oscillations of 12ω and 18ω. The harmonic pollution in each variable is the sum of the pollution of the components of 6ω, 12ω, and 18ω.

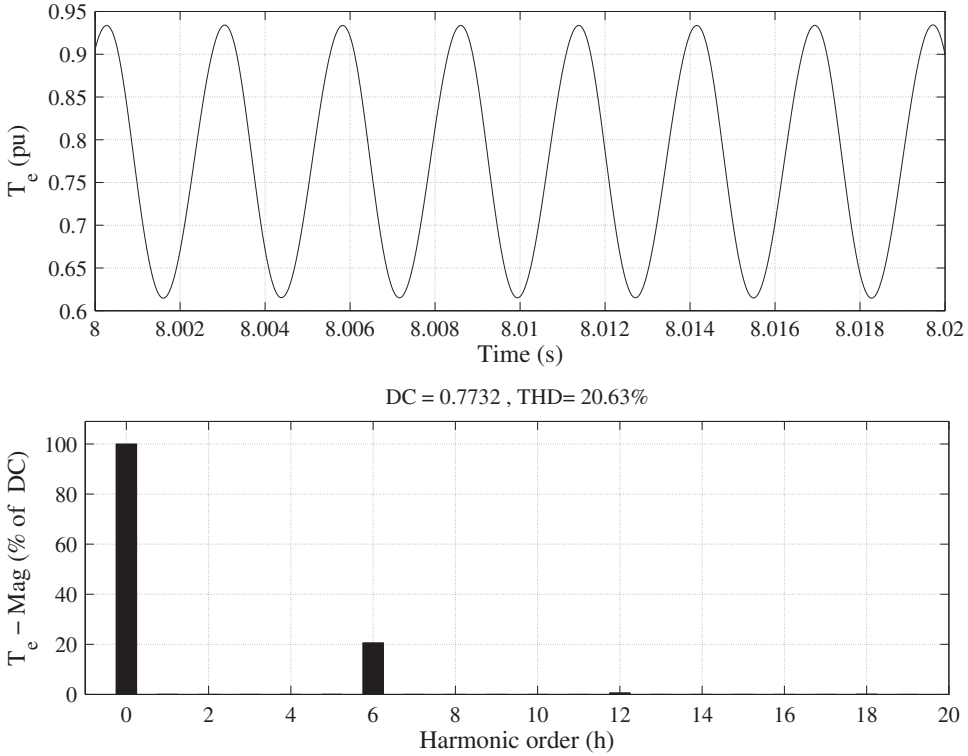

FIGURE 12 Electromagnetic torque oscillations and their harmonic spectrum

The behavior of the synchronous generator when it operates with the induction generator suppling a nonlinear load, possesses oscillatory disturbances in its electric variables. The electromagnetic torque pulsation is close to 21%, the effect on the generator is to heat up, due to the friction between the stator and the rotor caused by mechanical vibration and damage to the bearings.

The load angle also suffers alterations in nonsinusoidal steady state, the distortion in this variable is of ~18%. The currents induced on the damper windings together with the current induced on the field winding (oscillation of the excited current) will go on to cause superficial losses in the structure of the rotor, thus resulting in the heating of the rotor structure, in other words, ohmic losses in the rotor of the synchronous generator.

Noted also are very high oscillations in the quadrature and direct axis currents, also the oscillations on the quadrature and direct axis voltages should be considered as significant.

7.2 | Induction generator with a squirrel cage rotor

As the regime is nonsinusoidal, the electromagnetic torque has a pulsating nature, the pulsating electromagnetic torque and the harmonic spectrum of the electromagnetic torque developed by the induction generator are presented in Figure 21.

The quadrature axis stator voltage and its respective harmonic spectrum are presented in Figure 22.

The direct axis stator voltage and its respective harmonic spectrum are shown in Figure 23.

Keeping in mind that the frequency of these voltages is on the slippage frequency exerted by the induction generator, which is the fundamental frequency. In order to obtain the fundamental frequency, the relationship between the differences in mechanical speed of the induction generator to the synchronous speed are noted ($199.27 - 188.4956 = 10.7714$ rad/s). Through such one obtains the slippage frequency that is close to 3.4285 Hz for the harmonic load power used in the isolated system. Then the harmonic spectra of the electric variables, which are on the slippage frequency, are plotted.

The quadrature and direct axis stator current and its respective harmonic spectra are presented in Figures 24 and 25, respectively.

The quadrature and direct axis rotor current and their respective harmonic spectra are presented in Figures 26 and 27, respectively.

The harmonic components of the harmonic spectra are plotted as a percentage of the fundamental component, that is, in relation to the slippage frequency component.

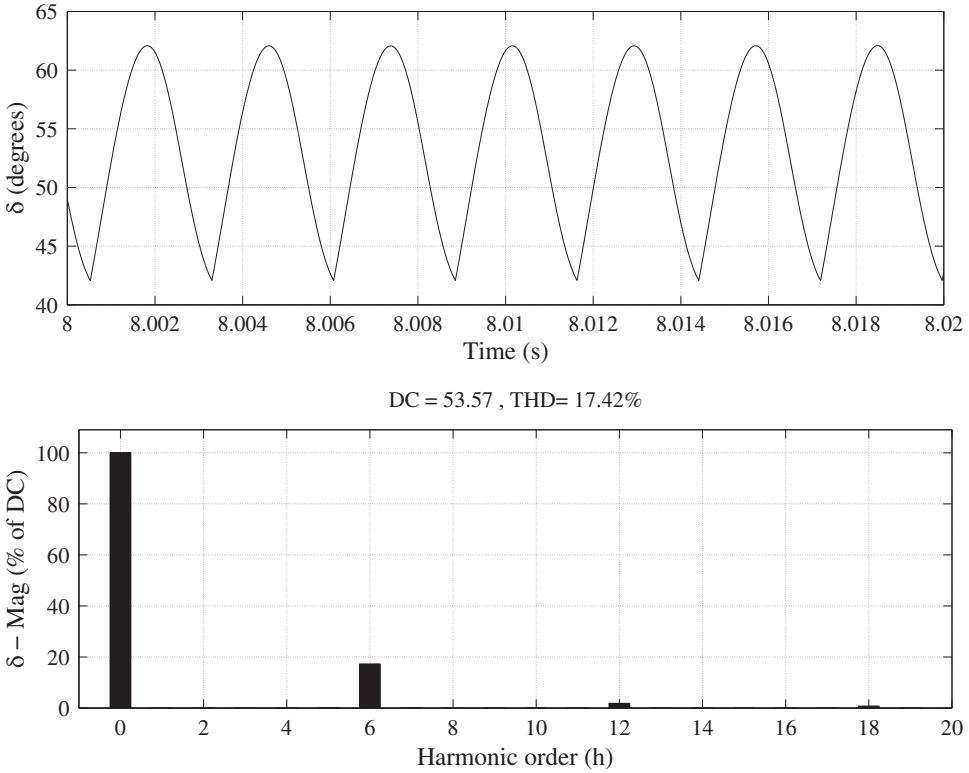

FIGURE 13 Oscillation of the load angle and its harmonic spectrum

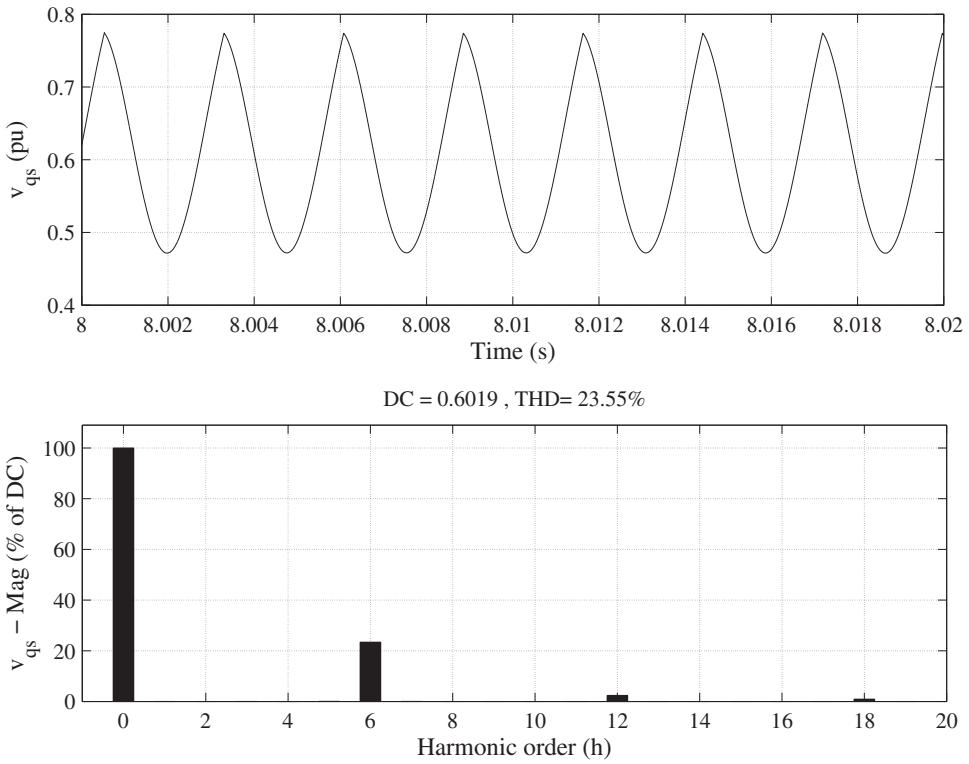

FIGURE 14 Oscillation of the quadrature axis stator voltage of the synchronous generator and its harmonic spectrum

By using Equation (11), one obtains $s_1 = -0.071599$. One finds s_5 and s_7 by applying the value of s_1 to Equations (18) and (19), respectively. Therefore, the values of the high slippage identified on the rotor of the induction generator are calculated by:

$$s_5 = -s_1 + 6 = 6.0571$$

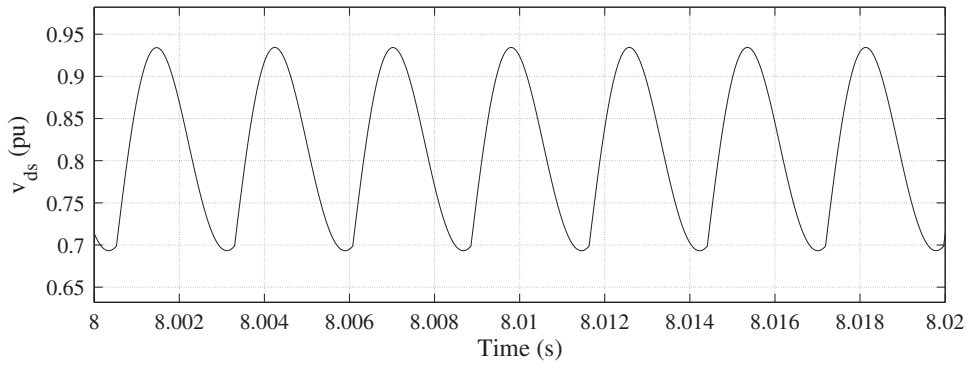

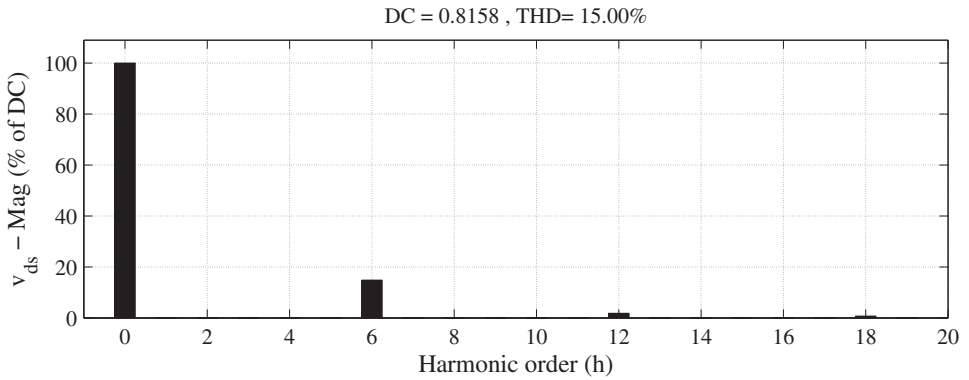

FIGURE 15 Oscillation of the direct-axis stator voltage of the synchronous generator and its harmonic spectrum

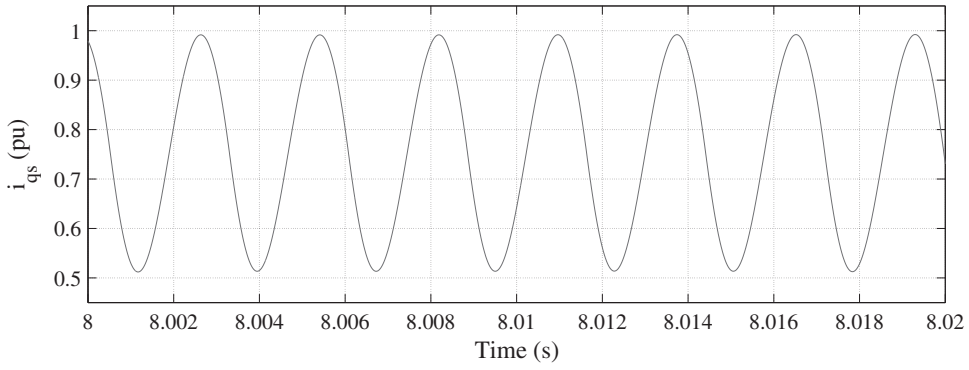

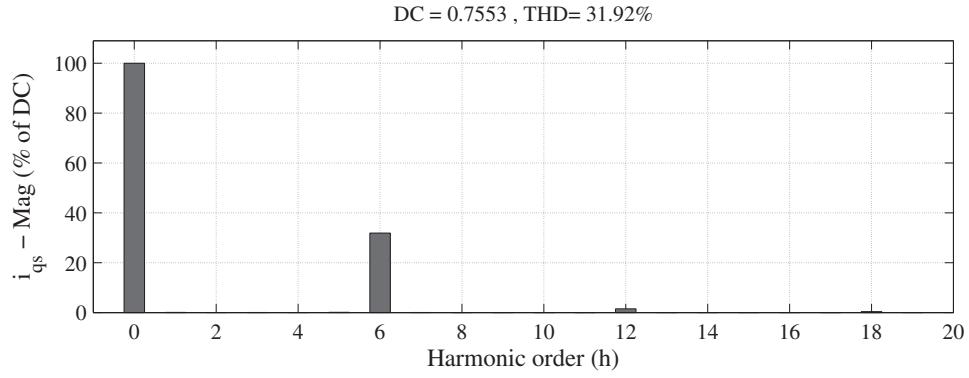

FIGURE 16 Oscillation of the quadrature axis stator current of the synchronous generator and its harmonic spectrum

$$s_7 = s_1 + 6 = 5.9428$$

Where the system frequency is 60 Hz, the fifth and seventh order frequencies on the slippage frequency will be of:

$$h = 5 \rightarrow 6.0571 \times 60 = 363.428\,\text{Hz}$$

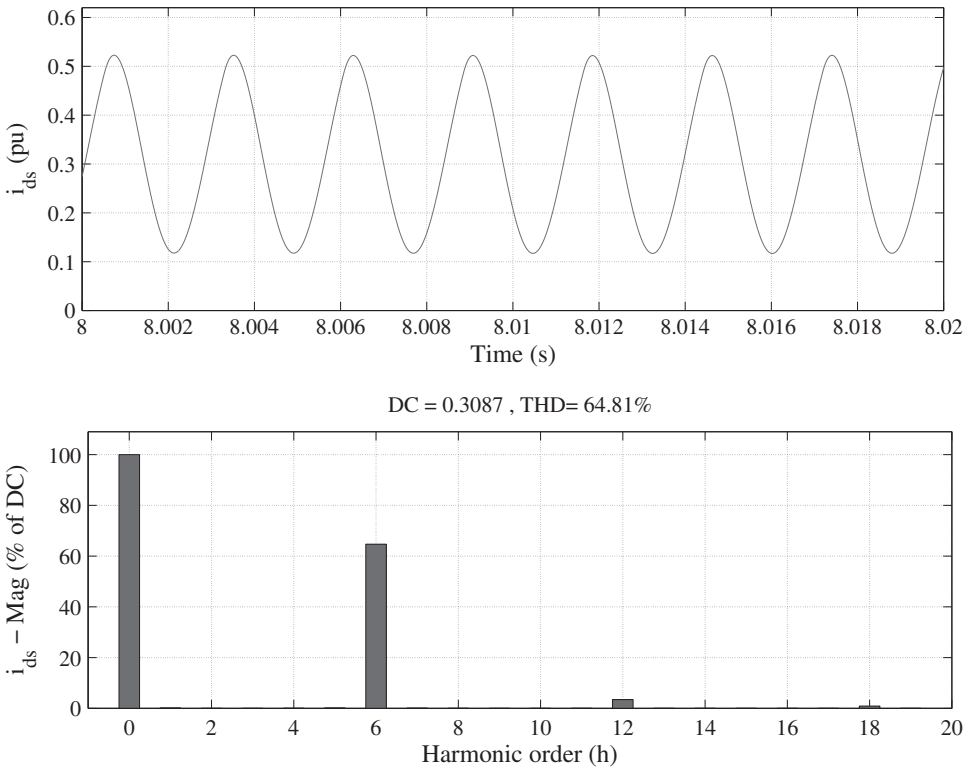

FIGURE 17 Oscillation of the direct-axis stator current of the synchronous generator and its harmonic spectrum

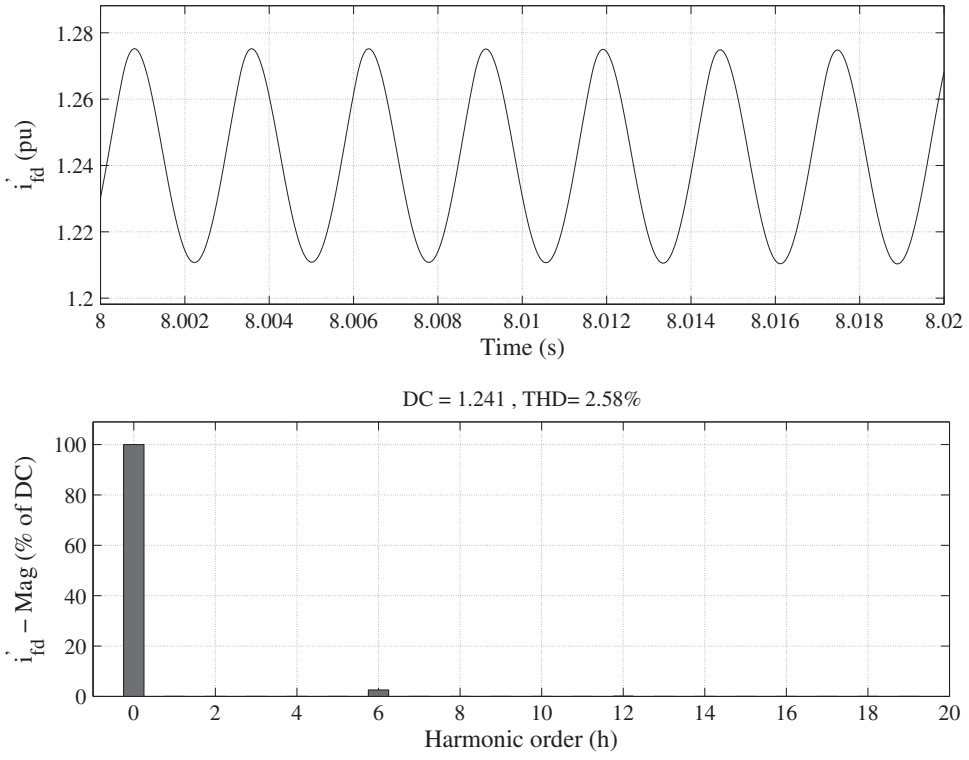

FIGURE 18 Oscillation of the field winding current of the synchronous generator and its harmonic spectrum

$$h = 7 \rightarrow 5.9428 \times 60 = 356.568\,\text{Hz}$$

For the higher harmonic orders, it is only necessary to make use of Equations (18) and (19) However, as noted from the above mentioned spectra, these are not expressive, this is due to the fact that the most significant harmonic components on the induction generator coils are of the fifth and seventh orders.

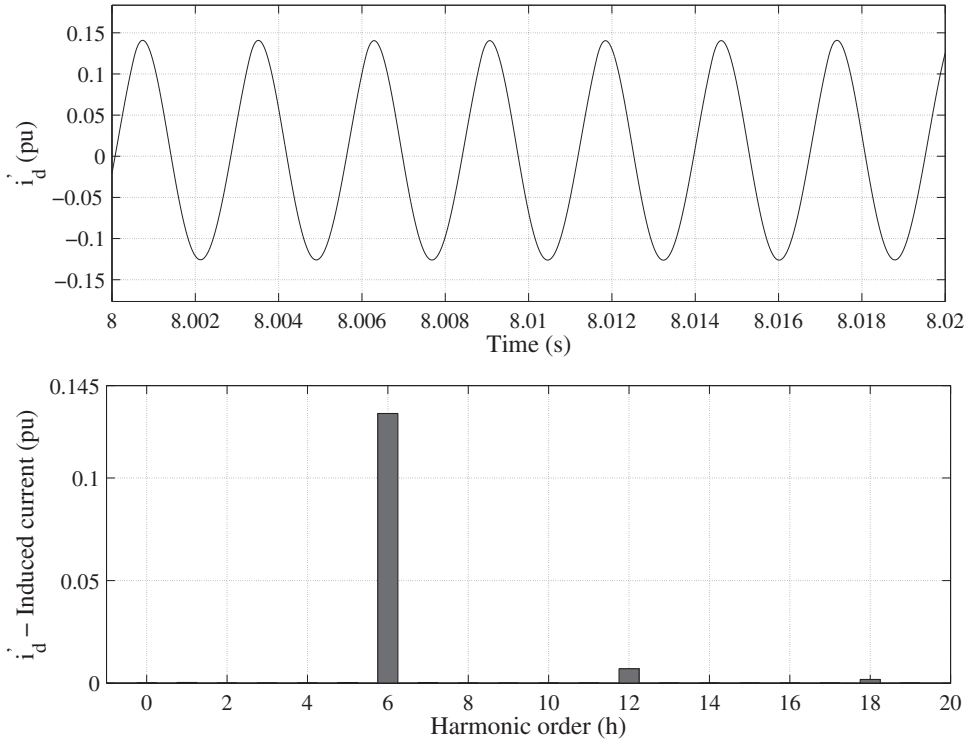

FIGURE 19 Induced current in the direct shaft damper winding of the synchronous generator and its harmonic spectrum

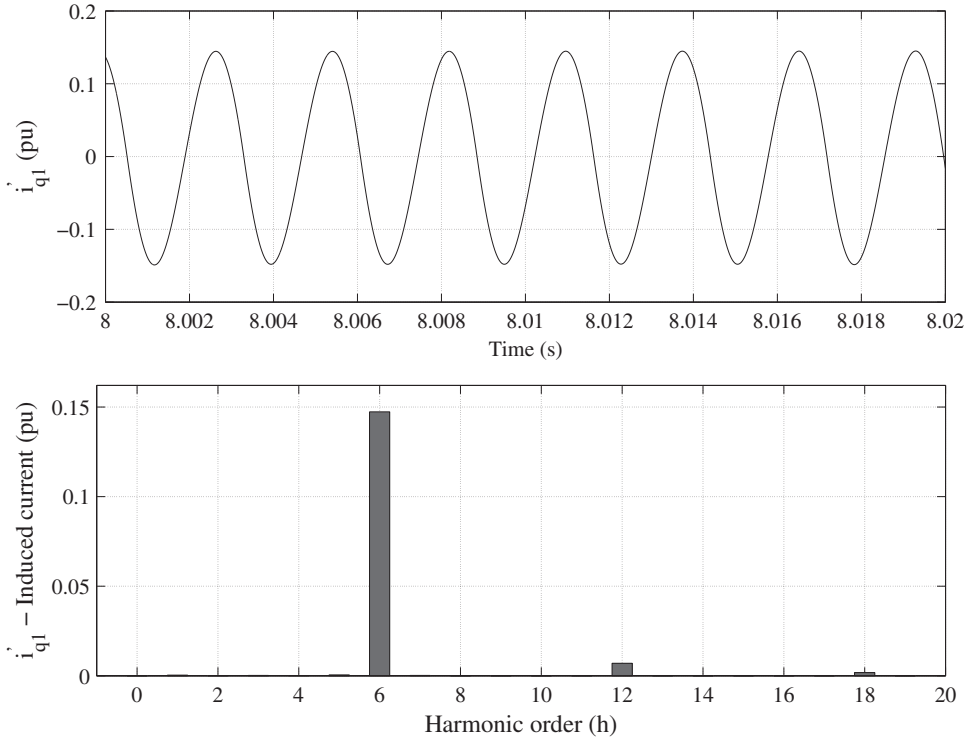

FIGURE 20 Induced current in the synchronous generator quadrature damping coil and its harmonic spectrum

Note that the oscillations of 6ω (360 Hz), 12ω (720 Hz), and 18ω (1080 Hz), can be seen around the harmonic components that approach these frequencies, on the respective harmonic components of positive and negative sequence from which it is composed. In other words, the seventh order and its multiples will be given in the harmonic slippage frequency of their respective positive and negative sequence harmonic orders.

As in the synchronous generator, oscillations are noted in the electric variables of the induction generator when supplying a harmonic load in parallel with the synchronous generator. Reiterating that the sixth harmonic component

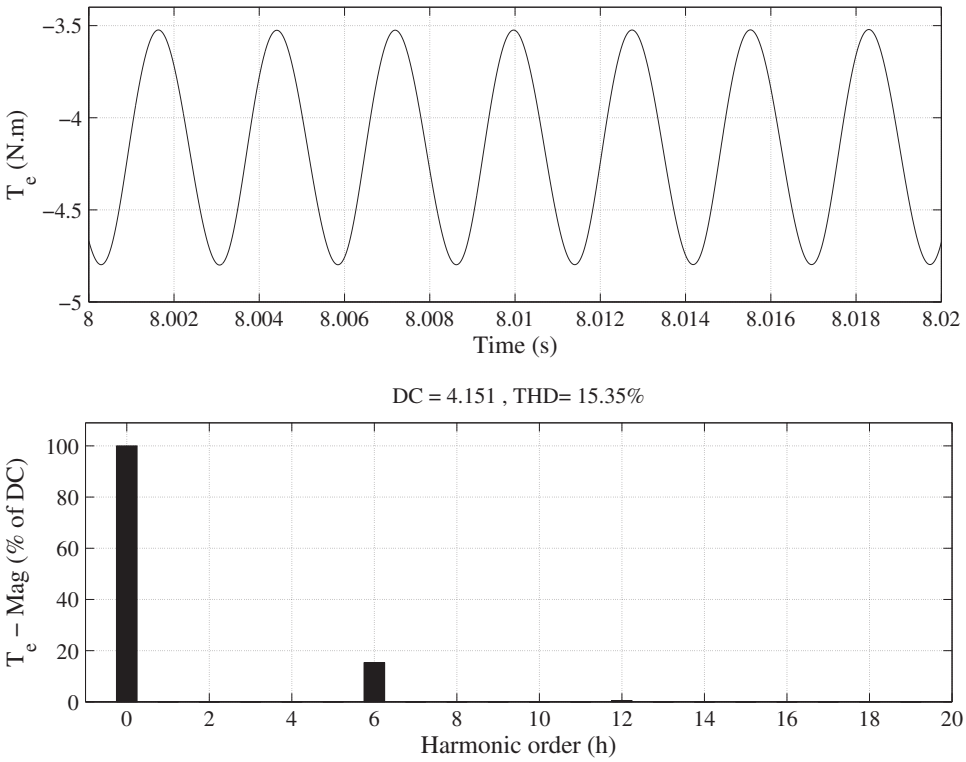

FIGURE 21 Oscillation of electromagnetic torque for the induction generator and its harmonic spectrum

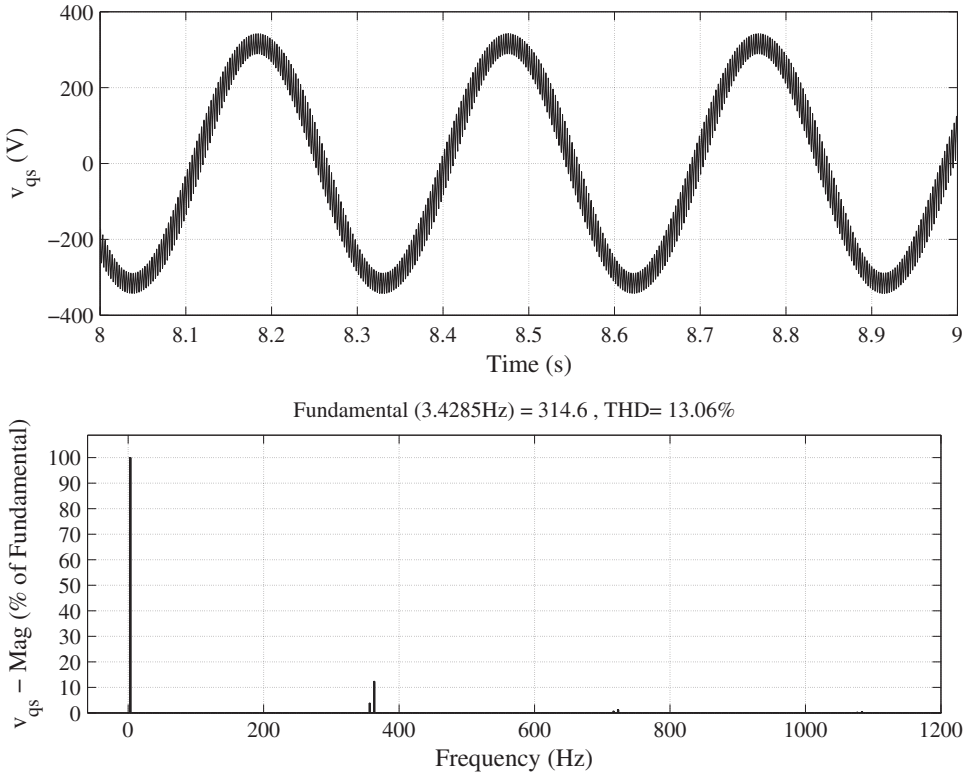

FIGURE 22 Oscillation of the quadrature axis stator voltage for the induction generator and its harmonic spectrum

is most predominant, due to the fifth and seventh harmonic order components being greater than those are that generate the oscillations of 12ω and 18ω for a three-phase rectifier, which is the nonlinear load. The total harmonic distortion on each variable is the sum of the pollution for the components of 6ω, 12ω, and 18ω. These oscillations vary according to the slippage/loading of the induction generator.

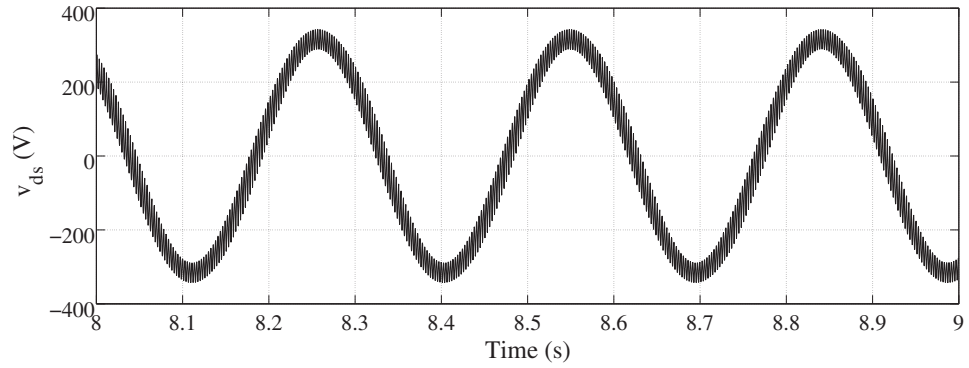

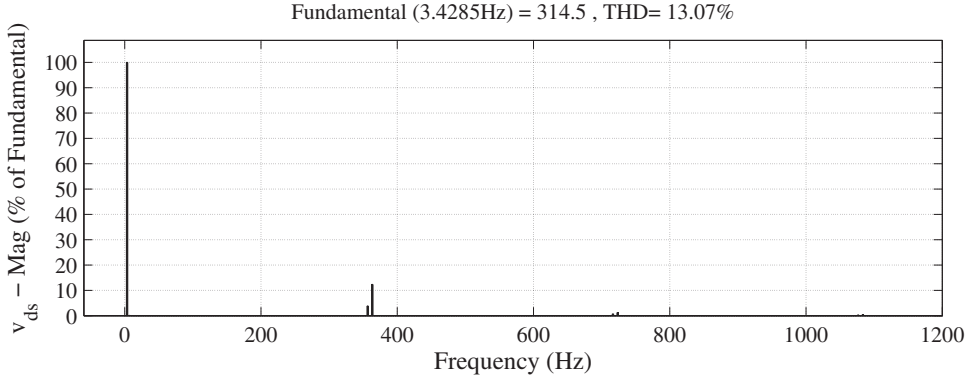

FIGURE 23 Oscillation of the direct axis stator voltage for the induction generator and its harmonic spectrum

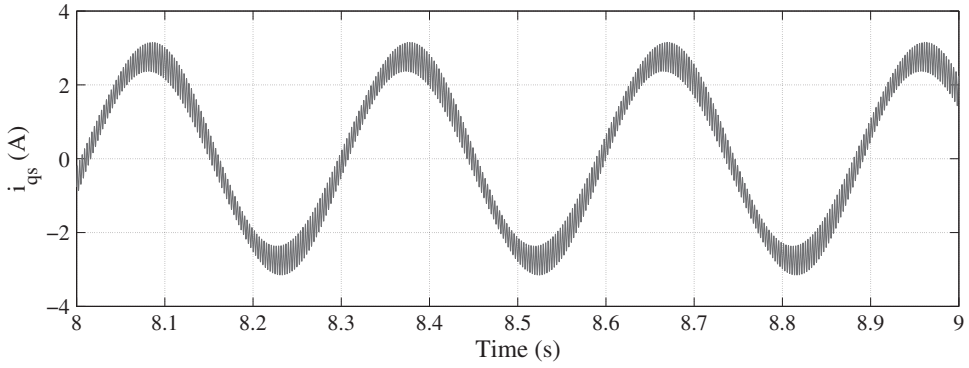

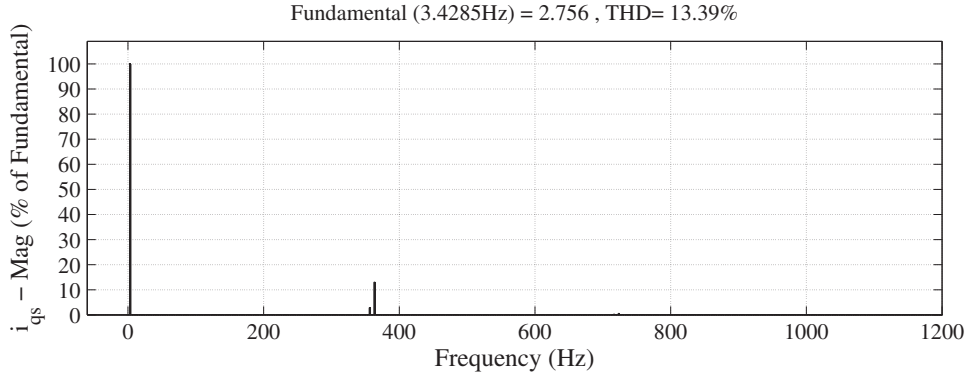

FIGURE 24 Oscillation of the quadrature axis stator current for the induction generator and its harmonic spectrum

The behavior of the induction generator when operating with the synchronous generator supplying a harmonic load, goes on to suffer disturbances in its electric variables as noted in the previously presented graphs. Although the electromagnetic torque pulsation of the induction generator is less than the synchronous generator, remaining around 16%, the effects will be significant and damaging to the structure of the generator.

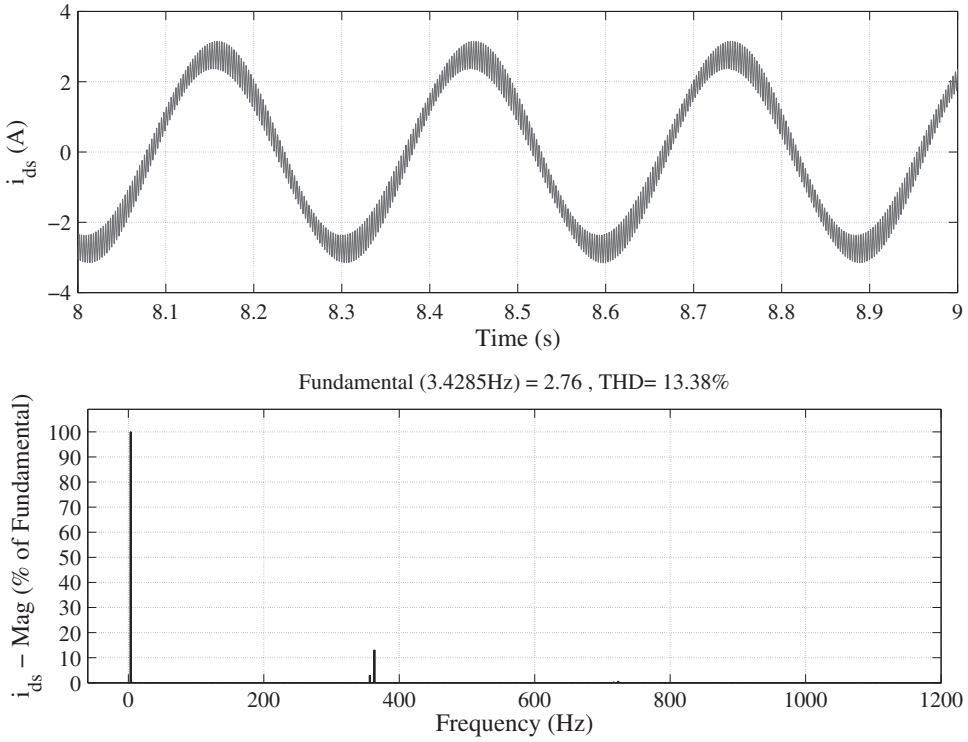

FIGURE 25 Oscillation of the direct axis stator current for the induction generator and its harmonic spectrum

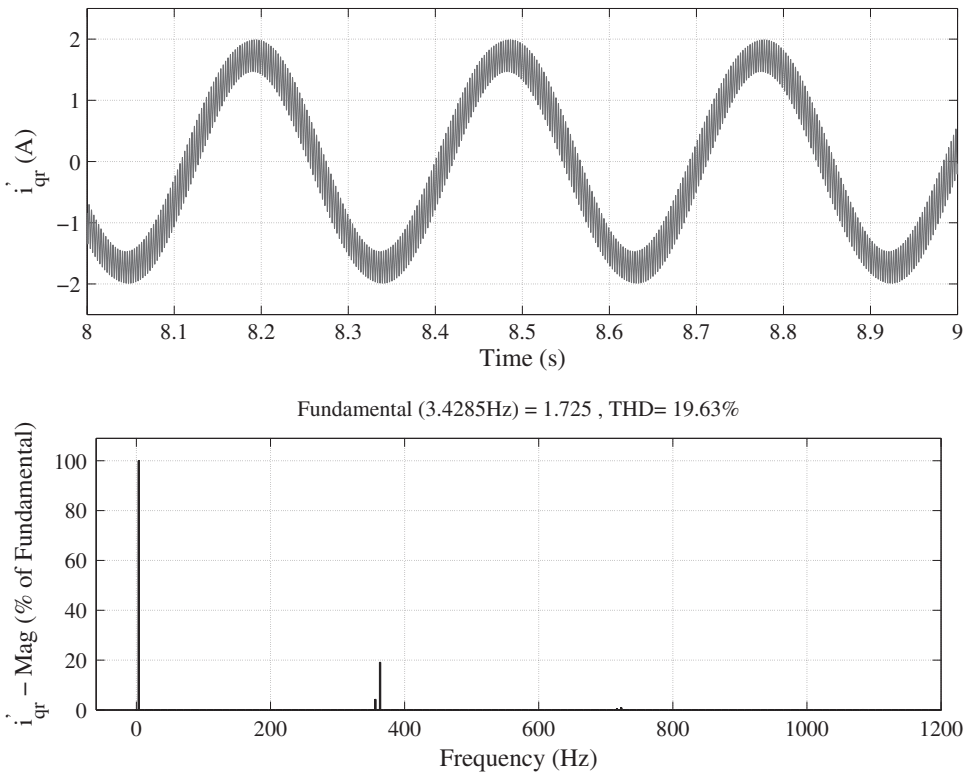

FIGURE 26 Oscillation of the quadrature axis rotor current for the induction generator and its harmonic spectrum

The disturbances on the electric variables end up resulting in the heating of the stator and rotor, besides dielectric stress in the air gap due to harmonic disturbances. These disturbances are principally found on the rotor, where the ohmic losses in the squirrel cage are considered greater in an asynchronous machine. These pulsating currents on the rotor result in electric losses on the surface of the cage, in addition to mechanical vibrations that the electromagnetic torque oscillations produce.

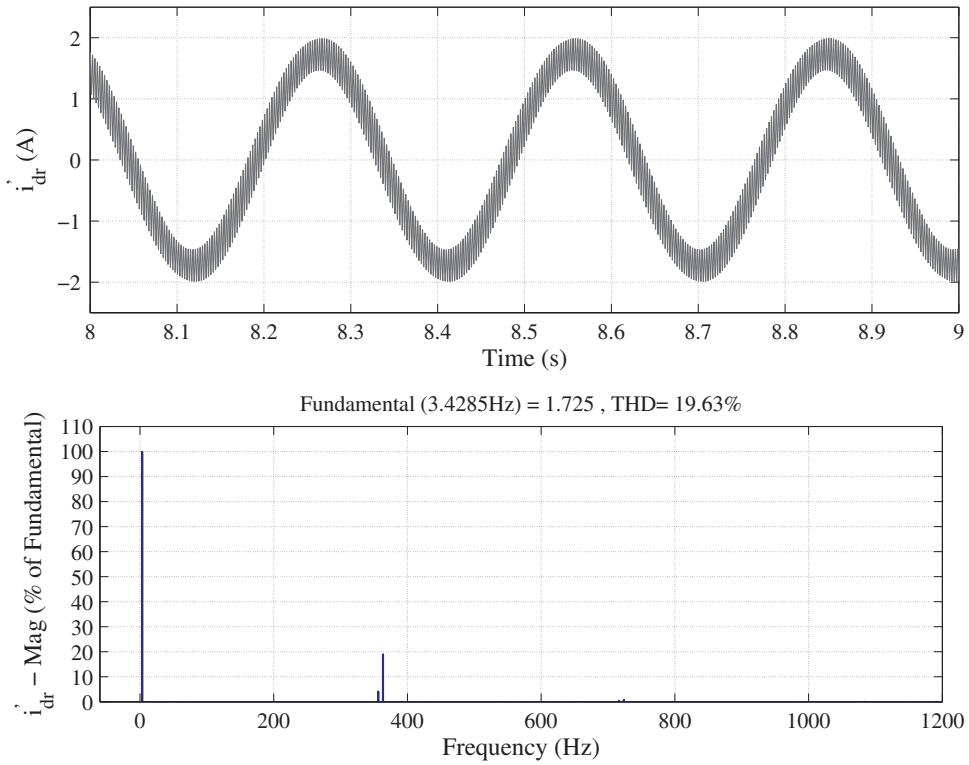

FIGURE 27 Oscillation of the direct axis rotor current for the induction generator and its harmonic spectrum

8 | ADDITIONAL COMMENTS

In a large isolated system, there exists an acquisition system for reading the generated voltage and current, as such it is possible to identify which are the harmonic components of higher density on the island system. In this way, it is easy to create the behavior modelling of harmonic pollution, as it can model by current or voltage source, if the impedance of the system is known.

Generator manufacturers make data and parameter for generators available, or experimental tests can be performed in order to obtain parameters, as well as the data for boards are normally described on the equipment. As such, it is possible by means of computational simulation to be aware of or analyze the effects on large systems, when an influence from harmonic pollution has arisen. Therefore, for any generator load with harmonic pollution, it is possible to perform the study be that in small or large plants.

In terms of turbo-generators, as these possess a lower inertia than a salient pole generator of the same power class, they possess greater oscillation of electromagnetic torque and as a consequence higher vibration and so greater will be the damage to the generator bearings, as well as producing a reduction to the working life of the generator.

Another factor to be considered is regarding the speed variation is when the turbo-generator is submitted to harmonic pollution:

In the same way that translation movement occurs on a body, where mass opposes speed variation, and as such needs an external force in order that this speed varies. In electric machines, in rotational movement, inertia opposes the variation of angular speed. Therefore, torque causes this speed to change, the speed variation causes an angular acceleration. As such, those machines of lower inertia tend to be more susceptible to speed variations. In this sense, due to the occurrence of oscillating torque, turbo-generators tend to suffer greater speed variation.

This line of research can be continued in harmonic mitigation on both generators. Thereby new techniques and techniques already used for harmonic attenuation can be implemented for harmonic mitigation on synchronous generators operating in parallel with squirrel cage induction generators in nonsinusoidal regime. Such publications[27-36] can be adapted to continue this research line for harmonic reduction in the isolated system proposed here.

9 | CONCLUSIONS

The disturbances caused by harmonic pollution in generators that operate in isolation are more expressive, as these are not connected to the electric system, whether these are in high voltage generation or in distributed generation. The

harmonic currents circulate only through a single circuit, which leads to a high voltage and current distortion, different to when connected to the infinite bus, where there exists harmonic escape onto the electric power system and the short-circuit level is high. Based on the experiments, it was possible to parameterize the simulation of the generators supplying a nonlinear load, the theoretical–experimental analysis, was shown to be close to the analysis of the oscillations on the electric variables of the generators.

Noteworthy in the synchronous generator is that the oscillations of 6ω, 12ω, and 18ω cause oscillatory disturbances on the electric variables. The pulsation of the electromagnetic torque in relation to its nominal value exceeds 20% oscillation, proving oscillations of mechanical torque, which results in mechanical vibrations, and consequently audible noise. The power angle oscillates above 17%, which can be lead to the synchronous generator losing stability, when up against the occurrence of sudden load switching, short-circuit, failures, among other eventualities in transitory state. The currents induced on the field and damper windings will go on to result in superficial losses on the rotor windings, which will result in heating and thus the elevation in rotor structure.

The disturbances on the induction generator are also expressive in their electric variables, due to harmonic pollution. Highlighted here is the electromagnetic torque oscillation that arrives close to 16% in relation to the continual nominal value, in the same way as the synchronous generator. This pulsating nature of the electromagnetic torque from the induction generator results in conjugate vibrations, which cause mechanical vibrations and consequentially audible noise. The currents induced onto the rotor of the induction generator, that being, on the squirrel cage, bring about oscillations over the current on the rotor in the slippage frequency that cause ohmic losses on the surface of the cage, resulting in heating and temperature elevation of the rotor structure.

The current distortion, in the generators, results in an increase of ohmic losses in relation to the *THDi* to the square of the stator windings, proving stator temperature rise.

The nonlinear loads are responsible for the generation of harmonics, due to the switching of nonlinear devices that employ power electronics. The study presented shows that when the synchronous generator operates in parallel with the induction generator in nonsinusoidal steady state, the disturbances caused by the harmonic pollution will reflect upon the behavior and operation of the generators, such as in yield reduction, loss of power factor, stator, and rotor heating. Such anomalies will reflect upon the increase of electric losses (thermal and dielectric stress) and mechanical damage (on the bearing structure) of the generators due to electromagnetic torque oscillations.

The study of disturbances caused by harmonic pollution in SPSG and induction generators that operate in parallel in isolated systems, demonstrates that it is possible to identify and quantify the oscillations on the electric variables of the synchronous generator and induction generator. Noteworthy here is that the oscillations of 6ω is the most expressive in the synchronous generator, and for the induction generator the resulting oscillations on the slippage frequency of the fifth and seventh order harmonics, due to the components of the fifth and seventh harmonic, will be higher due to the nature of the three-phase rectifier with a resistive load.

ORCID

Wagner E. Vanço https://orcid.org/0000-0003-1018-685X
Fernando B. Silva https://orcid.org/0000-0001-9859-6516
José M. M. de Oliveira https://orcid.org/0000-0001-7401-1149
José R. B. Almeida Monteiro https://orcid.org/0000-0002-5613-0096

REFERENCES

1. Sen PC. *Principles of Electric Machines and Power Electronics*. 3rd ed. Kingston, Ontario, CA: John Wiley & Sons; 2013.
2. Fitzgerald AE, Kingsley C Jr, Umans SD. *Máquinas Elétricas com Introdução À Eletrônica de Potência*. 6th ed. LTC; Porto Alegre: Bookman; 2006. 648p.
3. Wakileh GJ. Harmonics in rotating machines. *Electr Power Syst Res*. 2003;66:31-37. https://doi.org/10.1016/S0378-7796(03)00069-5.
4. I. Jadric, D. Borojevic, M. Jadric, A simplified model of a variable speed synchronous generator loaded with diode rectifier, in: PESC97. Rec. 28th Annu. IEEE Power Electron. Spec. Conf. Former. Power Cond. Spec. Conf. 1970–71. Power Process. Electron. Spec. Conf. 1972, IEEE, 1997: pp. 497–502. doi:https://doi.org/10.1109/PESC.1997.616769.
5. Nhut-Quang Dinh J. Arrillaga, a salient-pole generator model for harmonic analysis. *IEEE Trans Power Syst*. 2001;16:609-615. https://doi.org/10.1109/59.962404.
6. M. Ladjavardi, M.A.S. Masoum, S.M. Islam, Impact of time and space harmonics on synchronous generator load angle. Paper presented at: 2006 IEEE PES Power Syst. Conf. Expo., IEEE, 2006: pp. 1132–1138. doi:https://doi.org/10.1109/PSCE.2006.296468.
7. Tu X, Dessaint L-A, El Kahel M, Barry A. Modeling and experimental validation of internal faults in salient pole synchronous machines including space harmonics. *Math Comput Simul*. 2006;71:425-439. https://doi.org/10.1016/j.matcom.2006.02.003.

8. A.H. Samra, K.M. Islam, Harmonic effects on synchronous generators voltage regulation. Paper presented at: Proc. IEEE Southeastcon '95. Vis. Futur., IEEE, 1995: pp. 376–380. doi:https://doi.org/10.1109/SECON.1995.513121.
9. J.C.A. Escobar Martinez, F. de la Rosa, Shaft torsional vibration due to non-linear loads in low capacity turbine units. Paper presented at: 2001 Power Eng. Soc. Summer Meet. Conf. Proc. (Cat. No.01CH37262), IEEE, 2001: pp. 1403–1408 vol.3. doi:https://doi.org/10.1109/PESS.2001.970282.
10. N.G.M. Thao, K. Uchida, K. Kofuji, T. Jintsugawa, C. Nakazawa, A Comprehensive Analysis Study about Harmonic Resonances in Megawatt Grid-Connected Wind Farms. Paper presented at: 2014 Int. Conf. Renew. Energy Res. Appl., IEEE, 2014: pp. 387–394. doi:https://doi.org/10.1109/ICRERA.2014.7016415.
11. Liang S, Hu Q, Lee W-J. A survey of harmonic emissions of a commercially operated wind farm. *IEEE Trans Ind Appl*. 2012;48:1115-1123. https://doi.org/10.1109/TIA.2012.2190702.
12. Yang K, Bollen MHJ, Larsson EOA, Wahlberg M. Measurements of harmonic emission versus active power from wind turbines. *Electr Power Syst Res*. 2014;108:304-314. https://doi.org/10.1016/j.epsr.2013.11.025.
13. H. Kazemi Karegar, A. Shataee, Islanding Detection of Wind Farms by THD. Paper presented at: 2008 Third Int. Conf. Electr. Util. Deregul. Restruct. Power Technol., IEEE, 2008: pp. 2793–2797. doi:https://doi.org/10.1109/DRPT.2008.4523885.
14. S. Schostan, K.-D. Dettmann, I. Purellku, D. Schulz, Harmonics and Powers of Doubly Fed Induction Generators at Balanced Sinusoidal Voltages. Paper presented at: 2010 Int. Sch. Nonsinusoidal Curr. Compens., IEEE, 2010: pp. 213–217. doi:https://doi.org/10.1109/ISNCC.2010.5524482.
15. R.K. Mallick, S. Sinha, Improvement of power quality in a DFIG based wind farm using optimised Icosf DSTATCOM. Paper presented at: 2015 IEEE Power, Commun. Inf. Technol. Conf., IEEE, 2015: pp. 483–488. doi:https://doi.org/10.1109/PCITC.2015.7438214.
16. O. Ghatpande, K. Corzine, P. Fajri, M. Ferdowsi, Multiple reference frame theory for harmonic compensation via doubly fed induction generators. Paper presented at: 2013 IEEE Power Energy Conf. Illinois, IEEE, 2013: pp. 60–64. doi:https://doi.org/10.1109/PECI.2013.6506035.
17. Liu C, Blaabjerg F, Chen W, Xu D. Stator current harmonic control with resonant controller for doubly fed induction generator. *IEEE Trans Power Electron*. 2012;27:3207-3220. https://doi.org/10.1109/TPEL.2011.2179561.
18. Waluyo, S. Saodah, J. Nurahmat, Current Harmonic Analysis of Electronics Loads on Induction Generator. Paper presented at: 2012 IEEE Int. Conf. Cond. Monit. Diagnosis, IEEE, 2012: pp. 1167–1170. doi:https://doi.org/10.1109/CMD.2012.6416368.
19. Bento Silva F, Eduardo Vanco W, da Silva Goncalves FA, Junior CAB, de Carvalho DP, Neto LM. Experimental analysis of harmonic distortion in isolated induction generators. *IEEE Lat Am Trans*. 2016;14:1245-1251. https://doi.org/10.1109/TLA.2016.7459605.
20. Krause P, Wasynczuk O, Sudhoff SD, Pekarek S. *Analysis of Electric Machinery and Drive Systems*. 3rd ed. Hoboken, New Jersey, EUA: Institute of Electrical and Electronics Engineers, Wiley-IEEE Press; 2013.
21. S. Chattopadhyay, M. Mitra, S. Sengupta, *Electric Power Quality*, Springer Netherlands, Dordrecht, 2011. doi:https://doi.org/10.1007/978-94-007-0635-4.
22. *IEC 60034-1, IEC 60034-1: Rotating Electrical Machines – Part 1: Rating and Performance*. 11th ed.; Geneva, Switzerland: IEC Central Office; 2004.
23. J. Wang, P. Song, C. Cui, J. Li, T. Yang, Analysis of Operation of Synchronous Generator under the Distortion of Harmonic Current. Paper presented at: 2012 Asia-Pacific Power Energy Eng. Conf., IEEE, 2012: pp. 1–4. doi:https://doi.org/10.1109/APPEEC.2012.6307699.
24. Vanço WE, Silva FB, Monteiro JRBA, de Oliveira JMM, Alves ACB, Júnior CAB. Analysis of the oscillations caused by harmonic pollution in isolated synchronous generators. *Electr Power Syst Res*. 2017;147:280-287. https://doi.org/10.1016/j.epsr.2017.03.003.
25. Fuchs EF, Masoum MAS. Preface. *Power Quality in Power Systems and Electrical Machines*. Elsevier; 2008. https://doi.org/10.1016/B978-012369536-9.50001-2.
26. Chapallaz J-M, Dos Ghali J, Eichenberger P, Fischer G. *Manual on Induction Motors Used as Generators: A Publication of Deutsches Zentrum für Entwicklungstechnologien — GATE A Division of the Deutsche Gesellschaft für Technische Zusammenarbeit (GTZ) GmbH, 1° Edition*. Eschborn, HESSE, Germany: Springer Fachmedien Wiesbaden GmbH; 1992.
27. Zhao H, Wang S, Moeini A. Critical parameter design for a Cascaded H-bridge with selective harmonic elimination/compensation based on harmonic envelope analysis for single-phase systems. *IEEE Trans Ind Electron*. 2019;66(4):2914-2925.
28. Kim J, Lai J-S. Analysis of a shunt Wye–Delta transformer for multi-generator harmonic elimination under non-ideal phase-shift conditions. *IEEE Trans Ind Appl*. 2019;55(3):2412-2420.
29. Srndovic M, Zhetessov A, Alizadeh T, Familiant YL, Grandi G, Ruderman A. Simultaneous selective harmonic elimination and THD minimization for a single-phase multilevel inverter with staircase modulation. *IEEE Trans Ind Appl*. 2018;54(2):1532-1541.
30. Becker Tischer C, Tibola J, Giuliani Scherer L, Camargo R. Proportional-resonant control applied on voltage regulation of standalone SEIG for micro-hydro power generation. *IET Renew Power Gener*. 2017;11:593-602.
31. Fallows D, Nuzzo S, Costabeber A, Galea M. Harmonic reduction methods for electrical generation: a review. *IET Gener Transm Distrib*. 2018;12(13):3107-3113.
32. Singh B, Shridhar L, Jha CS. Improvements in the performance of self-excited induction generator through series compensation. *IEE Proc Gener Transm Distrib*. 1999;146(6):602.
33. "Harmonic elimination," in High Voltage Direct Current Transmission, Institution of Engineering and Technology, pp. 56–83.
34. A. S. Abdel-Khalik, M. I. Masoud, and B. W. Williams, Optimum flux distribution with harmonic injection for multiphase induction machine. Paper presented at: 5th IET International Conference on Power Electronics, Machines and Drives (PEMD 2010), 2010, pp. 213–213.

35. T. B. Kumar and M. V. G. Rao, Mitigation of Harmonics and power quality enhancement for SEIG based wind farm using ANFIS based STATCOM. Paper presented at: 2014 International Conference on Smart Electric Grid (ISEG), 2014, pp. 1–7.
36. E. Vargil Kumar, N. Pvrl, and S. Avrs, Steady state investigation of self excited 3 phase induction generator with novel leading VAR controller and mitigation of harmonics using active power filter. Paper presented at: *2010 IEEE International Conference on Power and Energy*, 2010, pp. 495–500.

How to cite this article: Vanço WE, Silva FB, de Oliveira JMM, Almeida Monteiro JRB. Effects of harmonic pollution on salient pole synchronous generators and on induction generators operating in parallel in isolated systems. *Int Trans Electr Energ Syst*. 2020;30:e12359. https://doi.org/10.1002/2050-7038.12359